Baddeley *et al.*
Progress in Earth and Planetary Science (2023) 10:53
https://doi.org/10.1186/s40645-023-00585-9

Progress in Earth and Planetary Science

REVIEW

Open Access

Space and atmospheric physics on Svalbard: a case for continued incoherent scatter radar measurements under the cusp and in the polar cap boundary region

Lisa Baddeley[1,3*], Dag Lorentzen[1,3], Stein Haaland[1,3], Erkka Heino[2], Ingrid Mann[2], Wojciech Miloch[4], Kjellmar Oksavik[1,3], Noora Partamies[1,3], Andres Spicher[2] and Juha Vierinen[2]

Abstract

Incoherent scatter radars (ISRs) represent the only instrument (both ground and space based) capable of making high temporal and spatial resolution measurements of multiple atmospheric parameters—such as densities, temperatures, particle velocities, mass flux—over an altitude range covering the entire mesosphere/lower thermosphere/ionosphere (MLTI) system on a quasi-continuous basis. The EISCAT Svalbard incoherent scatter radar (ESR), located just outside Longyearbyen (78.15°N) on Svalbard, is the only currently operating facility capable of making such measurements inside the polar cusp—an area of significant energy input into the atmosphere and characterized by heating instabilities and turbulence. The ESR was built in the mid-1990s and has provided valuable data for the international experimental and modelling communities. New radar technologies are now available, in the form of phased array systems, which offer new data products and operational flexibility. This paper outlines the achievements and current research focus of the ESR and provides scientific arguments, compiled from inputs across the international scientific community, for a new phased array ISR facility on Svalbard. In addition to the fundamental scientific arguments, the paper discusses additional benefits of continued ISR observations on Svalbard, building on the key findings of the ESR. Svalbard has a large network of complementary instrumentation both focused on the MLTI system (e.g. the Kjell Henriksen auroral Observatory, the Svalbard SuperDARN radar and the Svalrak sounding rocket launch facility) with synergies to other research fields, such as meteorology and oceanography. As a further holistic system science view of the Earth becomes more important, a new ISR on Svalbard will be important also in this respect with its ability to provide datasets with a wide range of scientific applications. Increased activity in space has highlighted problematic issues such as space debris. A changing Arctic has also seen increased human activity via the opening up of new shipping routes, which are reliant on GNSS technology that is effected by severe turbulence in the MLTI system. As such, societal applications of a future ISR are also presented. The accessibility and logistical support for such a facility is also briefly discussed.

Keywords Ionosphere, Atmospheric science, Space weather, Cusp, Polar cap, Plasma turbulence, Space debris, Incoherent scatter radar, Atmospheric escape

*Correspondence:
Lisa Baddeley
lisab@unis.no
Full list of author information is available at the end of the article

1 Introduction

The mesosphere/lower thermosphere/Ionosphere (MLTI) system extends from 60 to 600 km altitude and consists of a mixture of ionized and neutral gas components, the ratio between, chemical make-up and temperature of the two components varying as a function of altitude and latitude. Figure 1 shows a typical altitude profile of the ionized and neutral components of the atmosphere derived using the IRI-16 (Bilitza et al. 2017) and the NRL-MSIS 2.0 (Emmert et al. 2021) models. The ionized component (the density profile shown in Fig. 1, left hand panel) is directly controlled by electromagnetic forces, driven from above by interactions with the solar wind (the continuous stream of charged particles emanating from the Sun) and the Earth's magnetosphere (the region in the vicinity of Earth, where the ionized particle dynamics are controlled, in addition, by the geomagnetic field). The neutral component (the density profile of the main constituents is shown in Fig. 1, right hand panel), in comparison, is driven by the gas dynamics of the Earth's atmosphere from below. However, the tight coupling between the neutral and ionized component, can also result in both the forcing of the neutral atmosphere, due to the magnetospheric drivers, or the generation of ionospheric currents via neutral wind-driven processes. The partial ionization of the atmosphere at these altitudes also results in a separation of temperature profiles for the ionized and neutral components. These are shown in Fig. 1, middle panel. The above processes lead to a highly complex, dynamic system with energy and momentum deposition from both above and below causing atmospheric heating and chemical changes. The coupled nature of the atmospheric system resulting in these effects can also propagate deeper into the lower atmosphere. An additional source of energy is also present due to a continuous flux of cosmic dust and meteoroids which fall into the Earth's atmosphere. The ablation of meteors entering into the atmosphere leads to the formation of small solid particles, the meteoric smoke particles, which lead to changes in atmospheric chemistry.

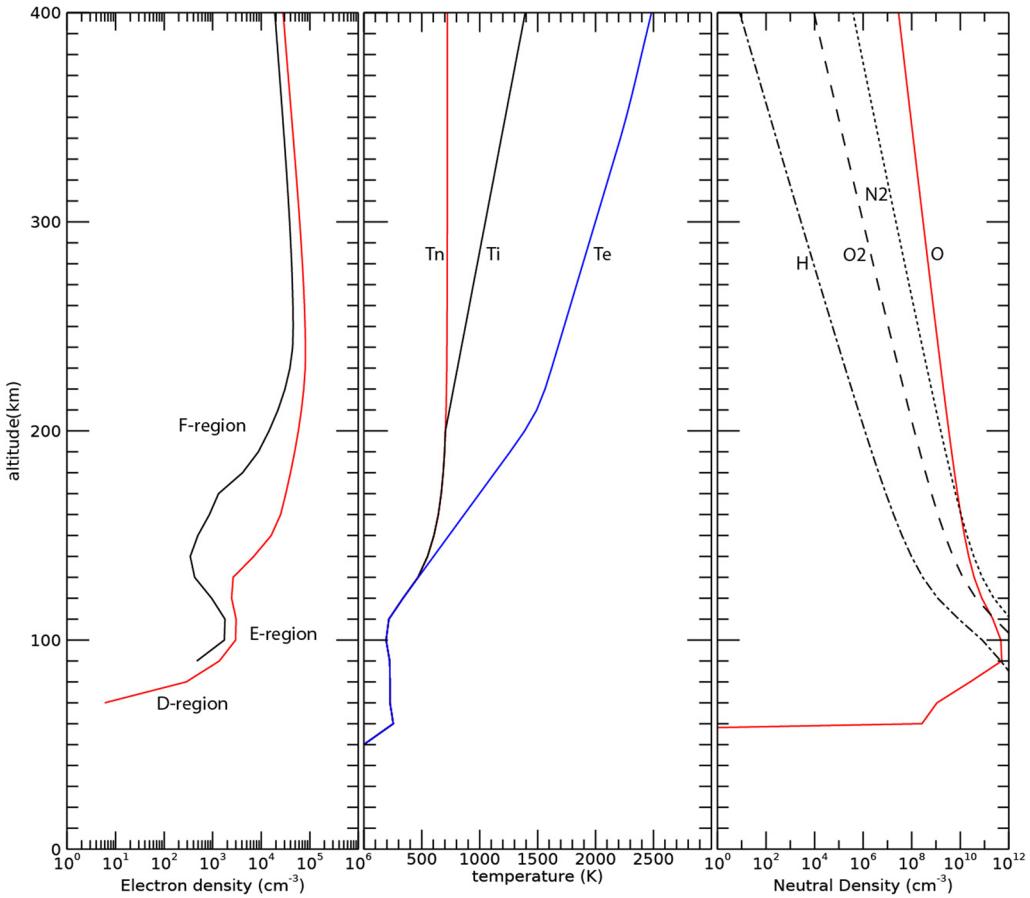

Fig. 1 Typical MLTI profiles over Svalbard in December. Left hand panel: Electron density profile at 1200UT (red) and 0000UT (black) using the IRI-16 model. Middle panel: Neutral (Tn), Ion (T) and Electron (Te) temperature profiles at 1200UT. Right hand panel: Neutral density profiles of various components, atomic oxygen (O), molecular oxygen (O2), molecular nitrogen (N2), atomic hydrogen (H) using the NRL-MSIS 2.0 model

The auroral zone, in the shape of an oval, is centred around ∼ 65° geomagnetic latitude at local midnight and ∼ 75° geomagnetic latitude at local noon. Poleward of this auroral zone is the polar cap region. Figure 2 shows these two regions schematically on a polar projection, MLT (Magnteic Local Time) plot with magnetic noon (12 MLT) at the top of the plot, dawn (06 MLT) to the right, dusk to the left (18 MLT) and midnight (00 MLT) at the bottom. This co-ordinate system is fixed with respect to the Sun, with the Earth rotating beneath it. In the figure, the fields of view of the proposed new Svalbard ISR and the EISCAT_3D system (discussed later in the document) are shown, together with some typical phenomena that are observed, and discussed later, in the polar ionosphere. Inside the polar cap and auroral zone, there are additional energy sources and coupling mechanisms to consider as the Earth's geomagnetic field is directly connected to that of the Sun (the Interplanetary Magnetic Field, IMF) which is embedded within the solar wind. The solar wind–magnetosphere–ionosphere connection results in a multitude of effects such as:

- Variation in the location and latitudinal extent of the auroral zone, and consequently the size of the polar cap.
- Driving of the ionized component of the Earth's atmosphere above ∼200 km into a global circulation pattern (shown as cyan contour lines in Fig. 2). The pattern's magnitude, direction and structure is associated with the strength and direction of the IMF. Momentum transfer between the ionized and the neutral atmospheric components then results in frictional heating and motion of the neutral atmosphere.
- Energetic particle precipitation into the MLTI system. The particles deposit their energy through ionization and dissociation of the atmospheric gasses generating a variety of auroral forms and localized heating effects. The penetration depth of the particles is determined by their initial energy resulting in

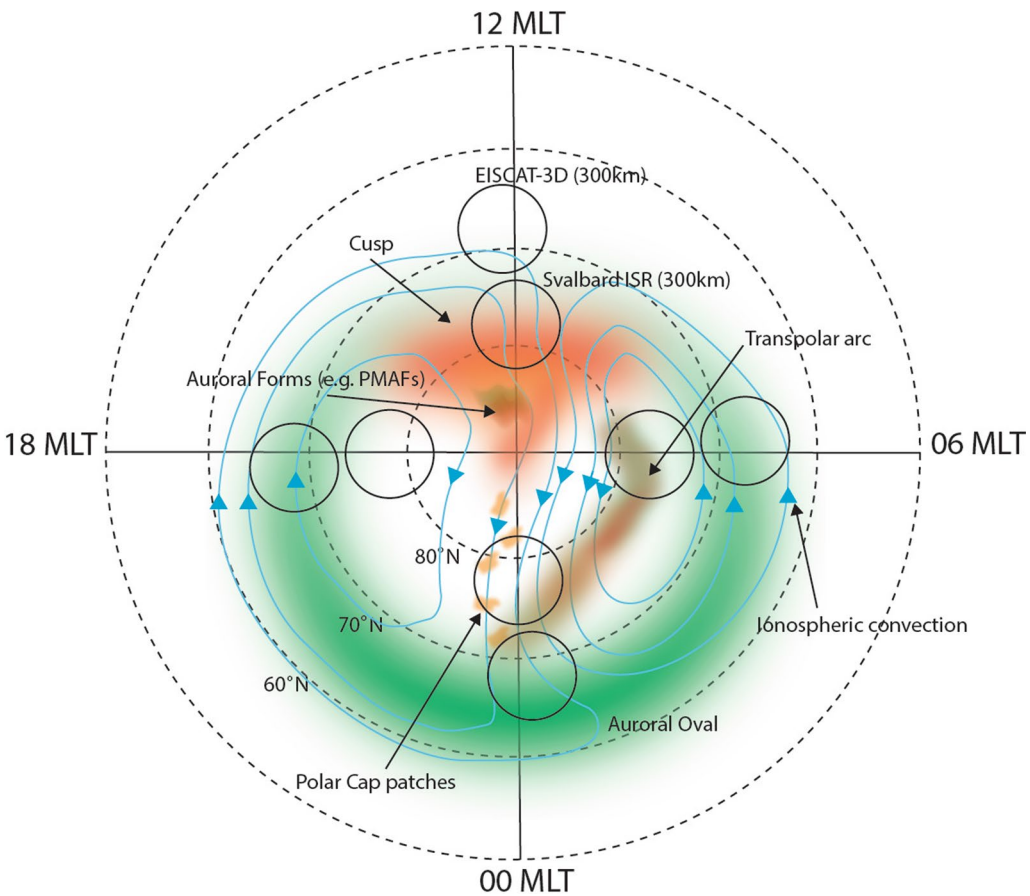

Fig. 2 Magnetic Local Time (MLT) plot showing the location of both the Svalbard ISR and new EISCAT_3D fields of view (at 300 km) (see Fig. 3) at 4 different MLT periods in relation to the main auroral oval and dayside cusp region. Other phenomena (such as polar cap patches) are also marked on for context

momentum transfer across the entire MLTI altitude range.
- Joule heating of the neutral atmosphere through horizontal current systems, set up as a result of current closure of field aligned (Birkeland) currents flowing along geomagnetic field lines.
- Loss of atmospheric mass via ion and neutral outflow, where material is transported upward along magnetic field lines from the ionosphere and into the magnetosphere.
- Creation of waves, instabilities and turbulence in the MLTI system. The resulting structuring of the plasma can span a wide range of temporal and spatial scales, from sub-second to hours and from hundreds of kilometres to scale-sizes of the order of the ion gyroradius (e.g. Tsunoda 1988).

An area of intense study by the research community is the magnetospheric cusps. These are two funnel shaped regions in the Northern and Southern Hemispheres where energetic particles from the solar wind have direct access to the Earth's magnetosphere and MLTI system. They are influenced by magnetic reconnection between the IMF and the geomagnetic field at the magnetopause; the dayside boundary of Earth's magnetosphere.

Once they enter into the MLTI system, the precipitating particles cause localized heating, turbulence and optical phenomena like the dayside aurora. The aforementioned global circulation pattern is initiated as a result of this reconnection process. The cusp also has relevance for low altitude polar-orbiting satellite missions as they experience a highly variable atmospheric drag effect as they pass through this region (Lühr et al. 2004). Although the reconnecting area at the magnetopause can be a few thousands km^2 wide, the resulting footprint in the MLTI system is relatively small (from less than 50 km in latitude to greater than 100 km in longitude, Fasel 1995; Moen et al. 1999; Newell and Meng 1992; Hosokawa et al. 2012), meaning there are only a few land-based locations, such as Svalbard and the remote interior of the Antarctic continent, where these phenomena can be observed through a combination of radar and optical instrumentation. At these high latitudes, there is no contamination from solar EUV due to the 24 h darkness conditions of the polar night (November–February in Svalbard) allowing processes in and around the cusp region to be studied unambiguously.

Another research area of increasing importance, especially in a societal context, is that of space debris. The polar regions are extremely well suited for observations of space objects, due to the frequent revisit period of objects with highly inclined polar orbits. At Svalbard, nearly every orbit of a polar orbiting space object will be above the horizon, ideal for precise measurements of orbital parameters. This is the same reason why Svalbard is one of the main ground station hubs for numerous satellite missions.

Over the last 5 years there have been several review papers (e.g. Sarris 2019; Palmroth et al. 2021; Heelis and Maute 2020) which have summarized the current understanding of the Earth's MLTI system. The papers have also highlighted the various knowledge gaps, instrumental and modelling challenges faced by the scientific community. An underlying theme is the need for (quasi-) continuous observations over the MLTI altitude range of key parameters like temperatures of the neutral and ionized constituents, conductivities, electric fields, neutral wind velocities and mass input that are necessary to quantify the energy input into the Earth's atmosphere. Such observations should be obtained over a multitude of spatial scales from kilometres to meters, and temporal scales from hours to sub-second. In this respect, there is only one instrument capable of stepping up to the challenge—a phased array incoherent scatter radar (ISR).

1.1 Incoherent scatter radars (ISRs)

ISRs have provided vital input to the exploration and understanding of Earth's middle and upper atmosphere since the technique was first proposed by Gordon (1958). Their importance and future role within scientific research was recently highlighted by a White Paper (Varney 2022) written in response to the National Academy of Sciences, Engineering and Medicine (US NASEM 2022) Decadal Survey 2023–2032. An excellent, more in depth review of the scientific contribution provided by these systems, in addition to a general science case for their continued use, is given by McCrea et al. (2015).

In recent (<10) years there have only been eleven such systems providing measurements of the MLTI system in routine operation (Sondrestrom, Aricebo, PFISR, RISR-N, RISR-C, Millstone Hill, ESR, EISCAT mainland, PANSY, MU and Jicamarca). Details of the radars can be found in Table 1. Aricebo was irreparably damaged and shut down in 2020 and Sondrestrom was shut down in 2018. Due to operational constraints, the PANSY radar only routinely provides data up to 90 km altitude (Sato et al. 2014). A new ISR system in China has just come (as of 2022) into operation at Sanya (Yue et al. 2022). Of these systems, there are five in the polar cap/auroral zone regions capable of making measurements across the full MLTI altitude range and only one in the vital cusp region—the EISCAT (European Incoherent Scatter) Svalbard Radar (ESR) (Wannberg et al. 1997). It forms part of the larger EISCAT network which also includes a UHF and VHF system in Tromsø, Norway as well as two remote receive sites in Kiruna, Sweden and Sodankylä,

Table 1 Incoherent scatter radar parameters

Name	Location (geographic latitude, longitude)	Operating frequency (MHz)
EISCAT Svalbard Radar	78°9 N 16°1 E	500
RISR (Resolute Bay) N/C	74°43 N 94°54 W	442
EISCAT Tromsø UHF/VHF	69°35 N 19°13 E	928/224
PFISR (Poker Flat)	65°6 N 147°28 W	449
MU	34°51′N 136°6 E	47
Millstone Hill	42°36 N 71°30 W	440
Jicamarca	11°57 S 76°52 W	50
PANSY	69°S, 39°36 E	47
Sondrestrom (shutdown in 2018)	66°59 N 50°57 W	1290
Aricebo (shutdown in 2020)	18°26 N 66°38 W	430
EISCAT_3D Transmitter site (operational from 2023 onwards)	69°20 N 20°18 E	223

Finland. The current EISCAT systems all rely on dish antennas (either a cassegrain or parabolic cylinder design) which can be tilted into position using a series of motors.

The more modern high latitude ISRs use a phased array design called AMISR (Advanced Modular ISR) (Valentic et al. 2013). These systems (which consist of thousands of smaller, dipole shaped antenna elements arranged in a grid formation) offer significant improvements in terms of both data coverage and operation. The arrays can be electronically steered into any pointing direction nearly instantaneously and are not reliant on one or several transmitters. The two polar cap AMISRs located in Resolute Bay, Canada (RISR 2022), and auroral region AMISR located at Poker Flat, Alaska (PFISR 2022), are all mono-static (meaning the transmitter is co-located with the receiver system) phased arrays.

The next generation of phased array ISR will be the EISCAT_3D system (EISCAT 2022), located in Northern Scandinavia, which is due to become operational in 2023. The system will replace the current EISCAT (Tromsø, Kiruna, Sodankylä) configuration in mainland Northern Scandinavia and will represent the first tri-static (one main transmitter/receiver site accompanied by two remote receiver sites) phased array radar in the world. The radar parameters are shown in Table 1. Mono-static systems, though highly effective, must make assumptions (for example, in regard to the mapping of electric fields along a magnetic field line) to derive some of the MLTI parameters. The tri-static capability will add a new dimension to the datasets as full 3D-vector quantities of the needed parameters will be obtained across a wide range of altitudes, latitudes and longitudes centred around the main auroral region (~65°). The field of view (fov), however, will not extend up to the latitudes of cusp region of the MLTI system (as can be seen from Figs. 2 and 3).

The ESR has made many significant contributions to the understanding of the Earth's atmospheric system, with a particular focus on the cusp region, since its inception nearly 30 years ago. One of the ongoing issues (in addition to wear and tear) is that, due to its growing age, replacement parts (such as transmitter klystrons) are almost impossible to obtain. It is thus envisaged that the radar is coming towards its end-of-life within the next 10 years.

In this paper we put forward a science case for a new phased array ISR facility on Svalbard. We consider incoherent scatter studies at high latitudes highlighting the essential part that the current ESR has played. We identify outstanding research questions for which high latitude and cusp ISR observations are essential. We discuss the benefit from having comparative observations at different latitudes and altitudes (including from other ground-based and space-based systems). We show how such a radar would be invaluable and also critical for future satellite missions by complementing their in situ measurements. There is a brief discussion regarding the design and location of a possible new ISR facility. We finally discuss the additional benefits (including logistical and collaborational) of maintaining such a facility on Svalbard, with its long history of ground-based research facilities across several different scientific disciplines.

2 Current understanding and knowledge gaps in the polar MLTI system

In the following sections, distinct research areas have been identified and discussed. It should be noted, however, that due to the highly coupled nature of the MLTI system many of the observed phenomena are intrinsically linked, i.e. polar cap patches (Sect. 2.2) travel with the background convection velocity and are often associated with auroral phenomena (Sect. 2.1) and plasma turbulence; ion outflow (Sect. 2.3) can be directly related to auroral features (Sect. 2.1). The different phenomena are shown schematically in Figs. 2 and 4.

2.1 Reconnection—convection, the polar cusp and auroral phenomena

The dayside cusp aurora is the product of the interaction between the solar wind and the Earth's magnetosphere through magnetic reconnection between the IMF and the geomagnetic field at the dayside magnetopause. A prerequisite for reconnection to occur is that a significant component of the two merging magnetic fields is anti-parallel to each other, creating a magnetic shear across the magnetopause. The evolution of the ionospheric footprint

of newly reconnected field lines manifests itself by the convective motion of the ionospheric plasma and in the dayside cusp aurora. At the magnetopause, this evolution is controlled by the dayside reconnection rate, giving rise to the magnetic tension forces and magnetosheath flows, whilst in the ionosphere, it is controlled by the conductive load at the end of the field line. The MTLI system in the auroral and polar cap regions are thus subject to this additional energy input in comparison to lower latitudes. Multi-spacecraft missions (CLUSTER, THEMIS, and MMS) have identified a wide range of transient phenomena in the upstream solar wind, at the bowshock, in the magnetosheath, and at the magnetopause. Hot flow anomalies, foreshock bubbles, magnetosheath jets, flux transfer events (FTEs), and surface waves are thought to play a significant role in the solar wind–magnetosphere–ionosphere coupling (Zhang et al. 2022). These phenomena are associated with the aforementioned variations in the IMF and solar wind dynamic pressure that deform the Earth's magnetopause. Much is still poorly understood regarding how magnetic reconnection plays out across the magnetopause. There currently exists no global dataset that describes the full 3D electrodynamics across the dayside magnetopause. However, the large areas of the magnetopause magnetically map to relatively smaller areas in the ionosphere (Newell and Meng 1992), and the phenomena manifest themselves through a variety of ionospheric signatures such as auroral precipitation and ionospheric convection, which can be measured by ground-based instruments, such as coherent scatter radars (CSRs) (e.g. The Super Dual Auroral Radar Network, SuperDARN, (Chisham et al. 2007; Nishitani et al. 2019) and ISRs. On a large scale (>500 km), plasma convection is recognized as having a general twin cell configuration with the plasma moving from the dayside cusp region, across the polar cap and into the nightside oval before flowing back to the dayside at lower latitudes (as shown schematically by the cyan lines in Fig. 2). This circulation is, to a high extent, determined by the IMF north/south orientation. For southwards directed IMF, magnetopause reconnection opens previously closed field lines convecting over the polar cap. This leads to an anti-sunward convection in the polar cap. For northwards directed IMF, lobe reconnection (on already open lobe field lines) sets up a sunward convection in the dayside polar cap. The large SuperDARN network provides observations of this large scale flow on a routine basis and has built up a database spanning over 25 years (e.g. Lockwood and McWilliams 2021). The large-scale auroral morphology is determined by the configuration of electrical currents that flow along magnetic field-lines, both into and out of the ionosphere. Dayside aurora is a result of such currents, where upward currents are carried by downward precipitation electrons. The dayside cusp aurora is typically produced by a high flux ($\sim$ 2–5 mW m^{-2} of low-energy (< 0.5 keV) electrons colliding with atomic oxygen at high altitudes (200–400 km), which in turn produces high intensity ($\sim$ 2–30 kR) oxygen optical emissions at 630.0 nm. The optical emissions are accompanied by thermal heating of the plasma and turbulence. The latitudinal/longitudinal extent of the cusp (e.g. Moen et al. 1999; Newell and Meng 1992) can provide vital information regarding reconnection processes at the dayside magnetopause. On scales smaller than this however, the flows can be turbulent and dynamic in nature and not fully understood (Lyons et al. 2016). The relative drift or velocity shears between the ionized and neutral components of the MLTI system also result in significant localized heating effects, although the dynamics and interactions between the two components is not fully understood. Studies using the ESR, in combination with other Svalbard instrumentation, have shown that the response time of the neutral component can vary significantly, depending on the auroral activity at a given time (e.g. Billett et al. 2020; Kosch et al. 2011). Statistical studies with the ESR have also shown an unexplained afternoon 'hot spot' which occurs at around 15 MLT (e.g. Cai et al. 2016). Whilst the magnitude of heating which occurs is statistically related to the polarity of the IMF, the smaller scale dynamics, including local auroral precipitation (and the field aligned current systems), are also thought to play a part (e.g. Aikio et al. 2002). Early radar observations using both CSRs and ISRs (Van Eyken et al. 1984; Goertz et al. 1985) reported flow signatures that were interpreted as ionospheric footprints of flux transfer events. Later, several types of poleward moving transients have been found, including flow channel events (Pinnock et al. 1993), pulsed ionospheric flows (Provan et al. 1998), poleward-moving radar auroral forms (Milan et al. 2000) and fast flow channels (Herlingshaw et al. 2020). A particular phenomena of reversed flow events, RFEs (Rinne et al. 2007; Oksavik et al. 2011) was discovered using the ESR indicating that the meso-scale ionospheric convection is often quite complex in the cusp and polar cap. ESR studies have shown multiple anti-parallel flow channels less than 50 km wide (e.g. Oksavik et al. 2004, 2005) embedded in the large-scale convection and of just a few minutes duration. Sounding rocket observations have also identified structured flows at 4–6 km scale (e.g. Oksavik et al. 2012).

In addition to the dynamic flows in and across the polar cap regions, there are a multitude of auroral structures and features. The different structures are indicative of different interactive processes and cover a huge variety of spatial (from 100 s km to 10 s m) and temporal (from hours to sub-second) scales. They can include

auroral arcs, proton aurora, cusp (dayside) aurora, poleward moving auroral forms (PMAFs), polar cap aurora and transpolar arcs, to name but a few. The polar cusp is identified as the 'source region' of several other phenomena such as ion upflow and neutral upwelling (see Sect. 2.3 of this manuscript). The link between upflow and the cusp has been investigated using the ESR in conjunction with both optical instruments (e.g. Moen et al. 2004; Lorentzen et al. 2007) and rockets (e.g. Burchill et al. 2010; Lund et al. 2012; Lessard et al. 2020; Moser et al. 2020). PMAFs are discrete auroral structures (Fasel 1995) which move polewards out of the cusp region at speeds that may exceed 500 m/s (Milan et al. 1999; Oksavik et al. 2005). They range in spatial extent from less than 50 km in latitude to greater than 100 km in longitude, occasionally, with time between successive PMAFs of less than 5 min (Fasel 1995; Hosokawa et al. 2012). PMAFs are related to changes in the solar wind but are often seen to occur spontaneously (Frey et al. 2019). They are associated with convection flow enhancements and turbulent small scale flow channels. ESR observations have revealed some of the complex nature of the energy deposition into the MLTI system by PMAFs (e.g. Skjæveland et al. 2011) as well as showing how they are related to other phenomena, such as polar cap patches (which are discussed later in Sect. 2.2 of this paper). The studies of dayside aurora and convection are thus vital for the understanding of the solar wind–magnetosphere–ionosphere interaction. There are several unanswered questions that are important in order to improve our understanding of this interaction:

- Is magnetic reconnection continuous in time or sporadic and over what time scales does it occur?
- Does reconnection take place in a single, large region of the magnetopause or rather in many smaller areas simultaneously?
- Are there ionospheric footprints that can reveal this—e.g. can PMAFs be used to infer the extent of the reconnection X-line?
- Why do PMAFs also occur during IMF northward conditions?
- How are dayside auroral forms affected by the magnitude and orientation of the IMF?
- What is the response time for dayside auroral phenomena in relation to the arrival of solar wind structures at the magnetopause?
- What role do the small scale plasma flows and auroral precipitation play in the formation of the afternoon hot spot?

In situ observations of such reconnection phenomena with spacecraft is challenging given the transient nature of the phenomena combined with the size of the interaction region ($\sim 10^{10}$ km^2). It would require hundreds (if not thousands) of spacecraft to make simultaneous multi-point observations of the magnetopause reconnection region. However, large areas of the magnetopause map magnetically to relatively small areas in the ionosphere (e.g. Moen et al. 1999; Newell and Meng 1992), and the phenomena manifest themselves through a variety of ionospheric signatures (such as auroral precipitation and convection), which can be measured by ground-based instruments, including ISRs.

Whilst the current ESR has made significant contributions to the research field, the observations are severely limited by temporal and spatial constraints due to existing observational data sets, e.g. one single radar beam direction, multiple discrete radar beams with poor angular and/or range resolution, or the maximum slew rate of a single radar dish. Consequently, it is difficult to fully characterize and quantify the full MLTI dynamics since assumptions must be made as to whether the phenomena under observation are undergoing temporal or spatial changes (i.e. is it multiple structures moving through the radar field of view or is it a static structure with temporal variations?). A new phased array radar in Svalbard would offer ground-breaking information to these fundamental questions through its ability to electronically point multiple beams. The new ISR will build on previous work looking at large scale flow bursts and FTEs (e.g. Nishitani et al. 1999; Fear et al. 2017) over an extended area along the dayside polar cap boundary. The combination of instrumentation allows the smaller spatial scale observations of densities, temperatures and velocities made by the ISR to be placed within the larger scale (>500 km) flow dynamics of the ionospheric system (measured by CSRs). The radar will be a pathfinder to pinpoint both the boundary itself, and the plasma motion across it (Lockwood et al. 2005). The new radar will give unprecedented measurements from the ground of how the instantaneous reconnection rate varies across an extended region of the dayside magnetopause. From its vantage point under the polar cusp, the new radar will provide trailblazing instantaneous monitoring of the footprints of multiple magnetic field lines along an area that potentially covers most of the dayside magnetopause, and from just one single radar site.

The proposed radar will also provide critical information on how plasma moves across the polar cap boundary. Outstanding questions to be addressed include:

- Is the momentum transfer spontaneous at the polar cap boundary, or does it vary with MLT in response to changes in IMF By?

- How long does momentum transfer continue into the polar cap, as the magnetic tension force pulls the magnetic field lines towards the nightside?
- What is the rotation rate of magnetic flux tubes, when there are strong shears in the convection due to a strong IMF By component?

2.2 Plasma instabilities, turbulence and ionospheric phenomena

The high-latitude ionosphere is known to be highly inhomogeneous, with the presence of "irregular" structures ('irregularities') and instabilities. These instabilities, which may lead to turbulence, generally occur when energy that has been stored unstably is redistributed (Baumjohann and Treumann 1997). The associated plasma structuring occurs over scales covering several orders of magnitudes from hundreds of kilometres to scale sizes shorter than the oxygen ion gyroradius (e.g. Kintner and Seyler 1985; Kelley 2009; Nishimura et al. 2022; Spicher et al. 2022). Assuming it can be described using fluid-like turbulence models (to what extend this is applicable remains an open question), it cascades from the energy source to the dissipation scales (Kintner and Seyler 1985). Characterizing high-latitude ionosphere should thus both address the sources of energy, i.e. the processes leading to turbulence, as well as the nature of the irregularities, i.e. the characteristics of the fluctuations and energy redistribution. Inhomogeneities in plasma density and electric fields are predominant near the cusp regions and around the auroral oval (e.g. Heppner et al. 1993; Jin et al. 2015, 2019), and fluctuations in density can impact the propagation of trans-ionospheric radio waves (e.g. Basu et al. 1988a; Bland et al. 2018) as well as signals from Global Navigation Satellite Systems (GNSS) (e.g. Carlson 2012; Jacobsen and Dähnn 2014). The study of such structures has thus significant importance for our technology infrastructure (e.g. Moen et al. 2013) and is discussed further in Sect. 2.5 Studies using current radar infrastructures, such as AMISRs, have helped advance our understanding of irregularity growth and decay as well as effects on scintillations, especially in the polar cap and auroral regions (e.g. Dahlgren et al. (2012); Forsythe and Makarevich (2018); Lamarche and Makarevich (2017); Lamarche et al. (2020); Makarevich et al. (2021); Lamarche et al. (2022); Semeter et al. (2017)).

ESR has contributed to better understanding of the high-latitude ionospheric plasma structuring at various scales (Kersley et al. 1988; Rinne et al. 2007; Carlson 2012). Thanks to its fortunate location under the cusp, where plasma enters the polar cap, it has been a pathfinder to shed light onto the formation and dynamic features of polar cap patches, which are localized areas of enhanced plasma density that are being transported with the large-scale convection pattern (e.g. Jin et al. 2019b; Oksavik et al. 2006; Moen et al. 2007). In fact, Carlson (2012) mentions that "Not until an incoherent scatter radar (ISR) measurements capability was created (...), was it possible to put the various mechanisms proposed for creating patches to a definitive test." The authors used mechanical scan modes to map the basic plasma parameters over a wide spatial area with temporal resolutions of just a few minutes (Carlson et al. 2002, 2004; Carlson 2012).

Polar cap patches (or more precisely gradients associated with them) are considered as one of the most important sources of small-scale irregularities in the polar cap at F-region altitudes (Tsunoda 1988). Patches are believed to be subject to the gradient drift instability (GDI) (Linson and Workman 1970; Simon 1963), which can cause density irregularities to grow and reach sizes of the order of the ion gyroradius (Tsunoda 1988) and kinetic scales (Gary and Cole 1983). Consequently, polar cap patches become increasingly more fine-structured as they travel across the polar cap (Weber et al. 1984; Gondarenko and Guzdar 2004), and may increasingly impact the trans-ionospheric propagation of radio waves. Additionally, in situ observations, using rockets, of a patch with km-scale gradients present already near its origin close to the cusp regions (Spicher et al. 2015) reinforced the view that other mechanisms, such as flow shears (Carlson et al. 2007) or particle precipitation (Kelley et al. 1982; Oksavik et al. 2012), may initially structure the patches, leading to multi-step processes.

Improving our understanding of polar cap patches, i.e. their creation, transport, and exit into the auroral oval, as well as the mechanisms responsible for their structuring is thus a crucial aspect for space weather mitigation (see Sect. 2.5) and to better understand development of turbulence in plasmas. Additional capabilities to monitor patches came with the phased array radars allowing to follow their formation and the associated cusp dynamics (Nishimura et al. 2021) and the structuring in 3D (e.g. Dahlgren et al. 2012; Forsythe and Makarevich 2018; Lamarche and Makarevich 2017; Lamarche et al. 2020). With Svalbard being ideally located just below the "patch entry" region (between 9 and 15 MLT) every morning, a phased-array system would provide invaluable information about patch creation and initial structuring, helping addressing questions that could not be resolved with a system providing observations in only one direction.

Polar cap patches are just one of the many dynamic phenomena that is believed to be important in the context of plasma structuring at high latitudes (Keskinen and Ossakow 1983; Kintner and Seyler 1985). Particle

precipitation and inhomogeneous flows (such as RFEs, detailed in Sect. 2.1) are fundamental features related to auroral forms (Oksavik et al. 2004; Moen et al. 2008) and commonly coincide with density irregularities (e.g. Basu et al. 1988b; Dyson and Winningham 1974; Kelley et al. 1982; Oksavik et al. 2011; Spicher et al. 2016, 2020). At macro-scales, F-region plasma structures may result directly from low-energetic particle precipitation (Moen et al. 2002; Kelley et al. 1982; Millward et al. 1999) or from instability processes in connection with field-aligned currents (Kintner and Seyler 1985; Ossakow and Chaturvedi 1979; Keskinen and Ossakow 1983). Inhomogeneous flows can, for instance, lead to shear instabilities such as the Kelvin–Helmholtz instability (KHI) (Keskinen et al. 1988) and to "stirring" (Kelley 2009; Burston et al. 2016) at large scales, and generate small-scale instabilities (Ganguli et al. 1994). Generally, the relative importance of the different mechanisms responsible for the formation and evolution of plasma irregularities (and whether the mechanisms actually occur) is not fully assessed. This is partially due to observational limitations, as current research infrastructures do not provide volumetric measurements of densities and fields covering all the scales involved, making it impossible to fully monitor both the sources and the irregularities (e.g. Nishimura et al. 2022). For instance, ESR "scans" combined with in situ data were recently used as representative inputs to numerical simulations of KHI (Spicher et al. 2020). It could be shown that KHI could structure the plasma quickly, however, the simulations could not be fully constrained because of "incomplete" observations, largely due to restricted resolution. Consequently, contributions (or lack of contributions) from other mechanisms such as GDI or precipitation could not be assessed. A new system providing volumetric and higher-resolution data would be necessary to evaluate the importance of the different mechanisms causing irregularities.

Testing turbulence theories also requires averaging over 3D volumes (Kintner and Seyler 1985). Currently, in situ studies of spectral characteristics associated with turbulence (e.g. Kintner and Seyler 1985; Ivarsen et al. 2019; Spicher et al. 2014, and references therein) provide merely information along the rocket or satellite trajectories. Having a system providing high-resolution multi-point measurement would help characterizing the nature of the structuring and the cascading of the energy across the scales, using for instance aspects from techniques such as those applied to meteor radars (Vierinen et al. 2019) or LOw-Frequency Radio interferometer ARray (LOFAR) (Mevius et al. 2016). For GNSS disturbances, scale-sizes of the order of a few hundred meters are crucial (e.g. Kintner et al. 2007). Furthermore, it has been shown that several of the relevant instabilities could possibly have fast growth rates (within minutes) (e.g. Makarevich 2016; Burston et al. 2016; Oksavik et al. 2012), with structuring evolving rapidly with time (e.g. Deshpande and Zettergren 2019; Spicher et al. 2022). Having a system encompassing the outer scales with resolution better than hundreds of meters (for GNSS related studies) and smaller with sub-second temporal resolution would thus be optimal.

A new phased array system on Svalbard would help address outstanding questions including (e.g. Nishimura et al. 2022):

- Which mechanisms are important for triggering plasma instabilities and forming ionospheric irregularities and when do they occur?
- How is energy distributed across different scales in the ionosphere? Which scales are dominant for given geomagnetic conditions?
- How does the energy cascade towards dissipation scales and which processes contribute most to heating of the MLTI system?
- How does the coupling within the MLTI system affect irregularity creation and decay?

Further significant advances are expected in the auroral regions using EISCAT_3D (McCrea et al. 2015). However, as highlighted in this manuscript, the cusp is a unique region in the MLTI systems where irregularities are also observed to peak (Jin et al. 2015, 2019a; Spogli et al. 2009). A new phased array system on Svalbard, working in tandem with the polar cap AMISRs (RISR-N and RISR-C) would increase the combined ISR spatial coverage and allow greater tracking of turbulence and irregularities as they move from their source region across the polar cap region.

A new radar, with an unprecedented spatial resolution across multiple latitudes and longitudes should also be able identify wave structures, which have their energy source both internal (through e.g. drifting particle populations, (e.g. Baddeley et al. 2005; Mager and Klimushkin 2008) and external (through e.g. Kelvin-Helmholtz wave signatures that propagate along the magnetopause (e.g. Rae et al. 2007; Samson 1991) to the Earth's magnetosphere. Observations using optical instrumentation have shown that the waves can structure auroral arcs (e.g. Rankin et al. 2021 and references therein) and produce multiple transpolar arcs (Zhang et al. 2020). ESR observations have also allowed the ionospheric heating and small scale field aligned current system associated with wave generated arcs inside the oval to be observed (e.g. Baddeley et al. 2017; Pitout et al. 2003). Modelling work investigating the structuring of the waves, along with the ionospheric response, such as energy dissipation rates

require high time resolution, altitude profile measurements of ionospheric conductivities and electric fields (e.g. Pilipenko et al. 2008; Fenrich et al. 2019). A new ISR, with a 3D volumetric imaging capability will be able to provide these.

2.3 Ion outflow and neutral upwelling

As an important supplier of plasma, the ionosphere possesses a significant influence on magnetospheric properties and processes. In the polar cap, due to the fact that the magnetic field lines are open to the solar wind, no hydrostatic equilibrium exists. Consequently, ions can be transported along magnetic field lines from the ionosphere to the magnetosphere (e.g. Chandler et al. 1991; Yau and Andre 1997). Ions of ionospheric origin, primarily H^+ and O^+, are characterized by low thermal energy of typically a few eV. The escape process is therefore often referred to as cold ion outflow, which can have a profound and direct effect on magnetospheric dynamics since a mixture of cold plasma and/or heavier ions like oxygen significantly alter fundamental plasma properties and instability thresholds in various regions of the magnetosphere (e.g. Yamauchi 2019; Toledo-Redondo et al. 2021).

Ion outflow is a consequence of ionization of the upper atmosphere combined with upward and outward transport, and thus depends strongly on local ionospheric conditions. Ionization is primarily driven by solar illumination and thus possesses a pronounced seasonal and diurnal variation (e.g. Maes et al. 2015; David et al. 2018). Upward motion of ions is initially driven by an ambipolar electric field set up by the difference in scale height between electrons and ions. Additional acceleration mechanisms such as the mirror force and the centrifugal force (e.g. Comfort 1988; Cladis et al. 2000) provide further energization. Near the cusp and auroral zone, additional ionization and energization mechanisms, including particle precipitation, Joule heating, quasi-static electric fields, and wave-particle interactions also operate (e.g. Dandouras 2021).

Enhancements in neutral density have also been observed at high altitudes (i.e. at 400 km and above) by a variety of spacecraft (e.g. CHAMP at $\sim$ 400 km and GRACE at $\sim$ 500 km (Kervalishvili and Lühr 2018). In the cusp region the neutral density is consistently enhanced at these altitudes by $\sim$ 35% (Kervalishvili and Lühr 2013) and has been likened to 'speed bumps' causing a deceleration in satellites passing thorough the region (Lühr et al. 2004). The enhancements have been linked to upwelling of neutral particles from the MLTI system. Suggested energization mechanisms are similar to those proposed for ion upwelling and outflow and the two are often seen to occur in parallel (e.g. Kervalishvili and Lühr 2013).

The ESR has provided valuable information on local ionization, which can be inferred from height profiles of electron and ion densities (e.g. Vickers et al. 2014; Bjoland et al. 2021). Upward acceleration due to the mirror forces depends strongly on the plasma temperature, which has also been derived from ESR measurements over a wide range of altitudes (e.g. Maeda et al. 2005). ESR measurements of the vertical ion velocity (e.g. Oyama et al. 2005; Yamazaki et al. 2017) have provided information about the initial upflow process set up by electrostatic fields. ESR observations also indicate that composition of the outflow can be assessed (e.g. Vickers et al. 2013). Likewise, recent studies using PFISR (Zou et al. 2017) have provided detailed observations of short lived, but highly dynamic ion outflow resulting from a sudden compression of the magnetosphere by the solar wind. Comparison with a global MHD model provided additional observational confirmation as to the validity of the model itself.

Due to their high orbital speed, low-altitude spacecraft in polar orbits can only provide snapshots of ionospheric parameters and processes of importance for ionospheric outflow. Observations of cold plasma above the exobase and in large regions of the magnetosphere are notoriously difficult due to spacecraft charging effects (e.g. Moore et al. 2016; André et al. 2021). Ground-based incoherent scatter radars do not suffer from these deficiencies. An ISR radar can thus provide crucial information to enhance our knowledge about ion and neutral outflow in polar regions. Outstanding questions include:

- What is the relative contribution to ion and neutral upwelling by Joule heating and soft particle precipitation in the cusp?
- What part does Alfvenic induced heating of the ionosphere play in enhancing the Joule heating rates?
- What is the role of local plasma conditions, such as temperature, density and vertical velocity, in ion outflow?

A challenge with the existing ESR is the limited signal-to-noise (S/N) ratio, in particular in the topside ionosphere (above the ionospheric F-layer). A higher transmitting power, better beam control, and strongly improved S/N ratio, which would be a possibility with a new phased array ISR facility, will overcome this problem and allow for a much better probing and characterization of the critical altitude range between the F-layer and the exobase.

2.4 Energetic particle precipitation, EPP

Energetic particle precipitation (EPP), where incoming protons and electrons have high energies of 1–1000 MeV,

and tens of keV to several MeV, respectively, can directly impact the Earth's mesosphere or upper stratosphere at altitudes as low as 30 km. The enhanced ionization caused by the precipitating particles leads to increased attenuation of radio waves and changes in the ion-chemistry and composition of the atmosphere. The effects on the neutral atmosphere can propagate down to the lower parts of the stratosphere and troposphere in the coupled atmospheric column.

ISRs are important for the studies of EPP and its effect on the coupled ionosphere-atmosphere system, as they are the only instrument type that can provide a direct measurement of ionization profiles during EPP. The ionization profiles are important for both ionospheric and atmospheric modelling as well as in studying the D region ionosphere (e.g. Tesema et al. 2022; Verronen et al. 2016). Ionization profiles or inverted spectra derived from radar data can be used in conjunction with satellites to investigate particle precipitation sources and the phenomena modulating the precipitating spectra (e.g. Miyoshi et al. 2015).

The enhanced ionization in the middle atmosphere caused by EPP leads to the creation of odd-hydrogen (HO_x) and odd-nitrogen (NO_x), which are both efficient at depleting ozone in catalytic reactions. In addition to destroying ozone where it has been produced, odd-nitrogen has a long lifetime in the polar night allowing it to descend inside the polar vortex down to approximately 30 km altitude where it can also deplete stratospheric ozone (Jia et al. 2020). Changes in the ozone concentration of the middle atmosphere lead to variations of the radiative and chemical balance potentially affecting tropospheric climate through dynamical downward coupling. This top-down mechanism, coupling energetic particle precipitation and the surface climate, is a possible source of natural regional climate variability in the polar regions (Gray et al. 2010; Seppälä et al. 2014), which can become more significant with climate change (Maliniemi et al. 2020).

EEP during substorms and pulsating aurora form a particularly important part of EPP that affects the ozone concentration (Andersson et al. 2014; Seppälä et al. 2015; Tesema et al. 2020; Verronen et al. 2021). Observations from incoherent scatter radars in the auroral regions have been used, for example, to study the source and precipitating spectra (Sivadas et al. 2017) of the electrons, EEP effects on the neutral atmosphere (Enengl et al. 2021), the spatial extent of the precipitation (Cresswell-Moorcock et al. 2013), and to create and validate precipitation models (Wissing et al. 2011).

Another category of EPPs is Solar Proton Events (SPEs). During SPEs the strongly increased ionization in the middle atmosphere reaches to lower altitudes which enables the use of ISRs to study the aeronomy of the middle atmosphere including, for example, the transition of charge from free electrons to negative ions and the effective recombination coefficient (e.g. Collis and Rietveld 1990; Collis 1996; Hargreaves et al. 1987, 1993; Verronen et al. 2006).

A new ISR located in the polar cap boundary region would be beneficial to complement the existing network of operational ISRs and EISCAT_3D at auroral latitudes. The long periods of polar night and midnight sun in the high Arctic, on Svalbard, enable studies of middle atmospheric phenomena that are affected by solar illumination in addition to EPP. An ISR in the polar cap would give information on the increased ionization that produces NO_x and HO_x within the relatively constrained atmospheric column of the stratospheric polar vortex during winter. These observations could be correlated and contrasted with satellite-borne observations of the concentration of these chemical species.

EPP at the latitudes of the polar cap boundary region is another important question itself. Due to fairly few detailed or long-term observations, many assumptions are typically made when discussing this topic. For SPEs a polar cap location could be used to study the uniformity of proton precipitation as a function of MLT and latitude (when contrasted with other observations from lower latitudes). An ISR close to the polar cap boundary is also perfectly positioned to study the contribution of high latitude pulsating aurora on the global EEP. These high latitude pulsating aurora events are almost only of the less energetic sub-type called amorphous pulsating aurora (Partamies et al. 2022). Furthermore, only by volumetric observations of electron density, will it be possible to resolve fine-scale precipitation within auroral structures, such as patchy aurora. A new ISR, on Svalbard, depending on placement and design (see Sect. 2.9 in regard to 'sea clutter'), would allow electron density profiles to be measured deeper down into the atmosphere, which would improve our understanding of both electron and proton effects in the high-latitude atmosphere. Some key unanswered questions on EPP include:

- What is the contribution of high-latitude EPP to the global energy deposition?
- How large is the electron contribution to the ionization during solar proton events?
- What is the role of spatial structuring of pulsating aurora in the precipitation energy?
- How does the lower atmospheric composition effect the ozone depletion during different EPP events?

2.5 Space weather forecasting

Many of the phenomena described in the previous sections can impact man-made systems which modern society is nowadays heavily reliant on. For example, signals from satellites orbiting around the Earth must pass through the MLTI region to reach a variety of receiver stations on the ground such as GNSS and communication devices. Structures and irregularities in the ionospheric plasma density, which are due to turbulence and instabilities, have been shown to impact the propagation of radio waves through wave diffraction and refraction. This leads to scintillation in the received signal, which in the context of GNSS, can result in positioning errors, or even loss of the satellite signal (e.g. Oksavik et al. 2015; Jin et al. 2019a; Moen et al. 2013; Prikryl et al. 2010; Semeter et al. 2017). In addition to navigation and positioning services, GNSS satellites are also used in other critical infrastructure such as a global time management for banking systems, financial institutions, power and communication networks. The ionospheric effects on the man-made infrastructure intensify during increased solar activity (which is often revealed through solar storms and coronal mass ejections (CMEs)), which can lead to geomagnetic storms. The associated strong ionospheric currents, energetic particle precipitations, or plasma irregularities can cause various problems such as HF blackouts (e.g. Bland et al. 2018), failures in power grids and loss, failure or shutdown of orbiting satellites (Ferguson et al. 2015) or previously mentioned disruption in the propagation of trans-ionospheric radio waves. Geomagnetic storms can also cause problems for directed drilling methods used by the oil and gas industry (Reay et al. 2005). These effects are all contained under the umbrella term 'Space Weather Effects', and many governments (e.g. USA (US Department of Homeland Security 2019), UK (UK Government, Dept of Business Innovation and Skills 2015), Canada (Government of Canada 2021)) and the European Union (EU Department of Defence Industry and Space 2021) have developed specific programs dedicated to the societal effects and mitigation plans in place in case of severe space weather events. Some estimates for different types of space weather events indicate a potential daily loss in the Gross Domestic Product from 6.2 to 42 billion dollars for the USA alone (Oughton et al. 2017). As such, there is considerable ongoing effort directed towards models which will have the ability to forecast space weather events, both in the long term but also, more importantly, the short term (so called nowcasting). A loss of sea ice (amongst other reasons) has meant increased activity (such as shipping and tourism) in isolated areas within the arctic regions. One aspect is related to navigation in complicated and shallow waterways where a small disruption or error in navigation or communication systems can have far reaching consequences. The ability for space weather forecasting with applications to more local, small scale regions in specific areas of the Arctic is thus also apparent. Studies have shown that the risk of systems experiencing positing errors is greater at high latitudes (Jacobsen and Dähnn 2014). This is also reflected in the global picture of ionospheric plasma irregularities and variability (Jin et al. 2019a). A recent report looking into risk and venerability around Svalbard (Governor of Svalbard (Sysselmesteren 2016)) specifically discusses space weather and highlights the need for further investigation. The ability for ISRs to provide full altitude profiles of densities and temperatures of the MLTI system has significantly increased our understanding both in terms of observations of specific space weather events but also in the context of providing data for, and developing physics-based and semi-empirical global and local space weather models. A new phased array ISR on Svalbard is vital for nowcasting and forecasting, as well as for modelling of space weather in the high latitude regions.

2.6 Meteoroid materials, polar mesospheric summer echoes (PMSEs), ice and dusty plasma

The flux of cosmic dust and meteoroids which enter the Earth's atmosphere has been studied using radars since the 1940s. The cosmic dust injection also influences incoherent scatter through the formation of small solid dust and ice particles predominantly in the lower parts of the MLTI system (the D-region ionosphere—see Fig. 1). These solid particles typically carry a surface charge and contribute to the overall charge balance in the ionosphere. The presence of dust is also considered to facilitate the formation of ice particles including sizes below the detection with optical observations. The cosmic dust injection finally contributes to the formation of atmospheric layers, including the PMSEs observed with radars that are also an important tracer of turbulence.

Meteor ablation is the loss of material from cosmic dust and meteoroids at the transition between mesosphere and thermosphere ($\sim$ 70 to 130 km). The free electrons that are generated in the process give rise to the headecho of the meteor (Pellinen-Wannberg 2005), which travels with the entering particles, and to the trail, which extends along the entering trajectory for some time. High power and large aperture radars, such as ISRs, allow observations of the headecho from high electron density region surrounding an ablating meteor (e.g. Kero et al. 2019, and references therein) and at the same time the conditions of the surrounding ionosphere (Pellinen-Wannberg et al. 2016). For a meteor radar, the advantage of a high latitude location is a better visibility of the high inclination portion of the meteor population which provides information on the orbital and collisional evolution of small

solar system objects. The main feature missing from the existing ESR system is that it suffers from sea clutter that reduces sensitivity to meteor headechoes, because both originate at a similar distance from the existing radar site. Additionally, the system cannot interferometrically measure the position of the meteor headecho within the radar beam, which prevents observing a trajectory or an unbiased radar cross section. Consequently, a future ISR should have interferometric capabilities.

The middle atmosphere contains ice and dust particles that are influenced in their dynamics by the neutral atmosphere and through charge interaction to the ionosphere, hence forming a dusty plasma. The ablation of meteors entering into the atmosphere leads to the formation of small solid particles: meteoric smoke particles. In summer the temperature near the mesopause at high and mid latitudes is so low that ice particles form, most probably through heterogeneous condensation onto the meteoric smoke. Satellite observations enable us to study some of the ice particles in Polar Mesospheric Clouds (PMC) at heights from 80 to 85 km (Hervig et al. 2001). These solid particles contribute to the overall charge balance. Through this they influence the chemistry which is mainly ion reactions at this altitude. Dust charging includes the attachment of electrons and ions, photoionization, photodetachment, and secondary ion emission. The first two processes depend on the conditions of the ambient ionosphere and also feedback to the ionosphere (Baumann et al. 2013). The long polar night allows investigations of the processes independent from those that are related to the solar photon flux. Finally, the electron precipitation couples to the charging through secondary electron emission (Baumann et al. 2016). The charged dust component influences the incoherent scatter observations (Rapp et al. 2013), and dust parameters are best retrieved under conditions of high electron content and in combination with independent measurement of the neutral temperature (Gunnarsdottir and Mann 2021).

The structure and occurrence rates of PMCs are latitude dependent and satellite observations have only limited capabilities to reveal characteristics such as their spatial structure (Gao et al. 2017), which is influenced by dynamic processes like upward propagating waves. The formation of PMCs and other coherent echoes is also linked to neutral atmosphere dynamics, because it involves its spatial structures. In addition, the mesospheric neutral temperature in the MLTI system is highly variable and causes formation and destruction of ice particles. The dust interactions are latitude dependent because they are influenced by ionospheric variability as well as global atmospheric circulation and turbulence in the neutral atmosphere.

Meteor ablation injects metallic ions into atmosphere and contributes to the formation of metal layers around 80 to 110 km including sodium, which is most extensively studied, but also iron, potassium, calcium and magnesium layers (e.g. Plane et al. 2015). The ice particles also contribute to the formation of PMSEs. A topic of ongoing research is to find out whether meteoric smoke particles also contribute to the formation of coherent radar echoes that are observed during other times of the year, i.e. Polar Mesospheric Echoes or Polar Mesospheric Winter Echoes (Latteck and Strelnikova 2015).

The main questions of scientific interest are:

- What is the influx of meteoric matter into the Earth's atmosphere?
- What is the distribution of orbital elements, composition, and sizes of meteoroids that cross the Earth's orbit?
- What are the consequences of meteoric matter to the Earth's atmosphere?

2.7 Space debris

Space is a valuable resource with wide-ranging societal and economical impacts. Earth orbiting satellites are crucial for environmental monitoring, navigation, and telecommunication. In the future, satellite services will be the most cost effective way of connecting half of the world's population to the internet. The number of man-made objects in Earth orbit have steadily increased during the last 50+ years. The threat of a collisional cascade chain reaction unfolding in space was identified by Kessler and Cour-Palais in 1978 (Kessler and Cour-Palais 1978; Kessler et al. 2010). In 2020, there were estimated to be approximately 10^6 objects over 1 cm in diameter in Earth orbit (Horstmann et al. 2021) and several orbital regions may have already passed the critical density where the collisional cascade chain reaction will start increasing the number of objects even if no new objects are launched.

The outlook for the future is challenging for humanity. The number of objects in space will keep increasing due to new launches and fragmentation events such as collisions and explosions occurring in space on a fairly regular basis. Recently, it has also been suggested that atmospheric drag experienced by spacecraft will be reduced in the future due to changes in radiative transfer caused by increased atmospheric CO_2 content in the Earth's troposphere, followed by subsequent cooling in the topside atmosphere. This will cause significant increases in orbital lifetimes of space debris objects, which will further exacerbate the situation.

Continuous monitoring and development of more tracking capacity are the primary means of mitigating the risks associated with the increased number of hazardous

space objects. Observations with ground-based radars are the most important method for characterizing the population of space objects in Earth orbit (Klinkrad 2006). This includes calibrating statistical models of space debris (Flegel et al. 2009; Krisko 2014) using beam-park surveys, as well as maintaining a catalogue of orbital elements for specific objects. At the moment, the US Space Command maintains the largest catalogue, which contains approximately 25,000 objects. This only covers a small fraction of the > 1 cm diameter objects, which are thought to be potentially hazardous.

The IPY dataset obtained by ESR between 2007 and 2009 was used to study the evolution of space debris as a secondary data product derived from the ionospheric radar experiment (Markkanen et al. 2009). This measurement period also coincided with the Chinese anti-satellite experiment in January 2007, allowing studies of distribution and evolution of the resulting space debris to be made. Since then, EISCAT radar measurements have played an important role in characterizing the space debris produced by several other major fragmentation events, such as the 2009 Iridium-Cosmos satellite collision (Vierinen et al. 2009) and the 2019 Indian anti-satellite experiment. Validation of statistical space debris models relies on regular beam-park radar observations.

An ISR is typically useful for characterizing objects with diameters approximately larger than 0.1λ, (where λ is the radar wavelength), as smaller objects will be in the Rayleigh scattering regime with significantly reduced radar cross sections. The 60 cm wavelength of the existing ESR system is already relatively well suited for tracking even smaller size debris, but the smallest diameter of potentially hazardous objects will still be outside of reach due to a too small radar cross section.

The primary physical parameters that a radar system would need for observing space debris is an unbiased observation of the radar-cross section, as well as the ability to make observations of the trajectories of objects. None of the existing EISCAT systems have these capabilities at the moment. There are two ways to technically achieve these goals: 1) using a tri-static measurement geometry like EISCAT_3D (Vierinen et al. 2017), or 2) using interferometric angle of arrival determination. The second option has the advantage that it can be accomplished with just one radar site.

One possible synergy with a space object tracking capable radar in Svalbard is that it can be used for diagnostics and launch support for future spacecraft launches from Andøya Space Port.

2.8 Supporting infrastructure

Svalbard provides a unique location, with the long polar night (nearly three months of 24 h of darkness), ideal for the ionospheric cusp to be easily identified by ground-based radars and optics. The darkness allows for its effects to be easily separated from those due to solar EUV radiation, something that is logistically, extremely challenging to do with multiple ground-based instrumentation anywhere else on the globe. Consequently, Svalbard has a long history of ground-based MLTI measurements, starting with the first international polar year in 1882–1883.

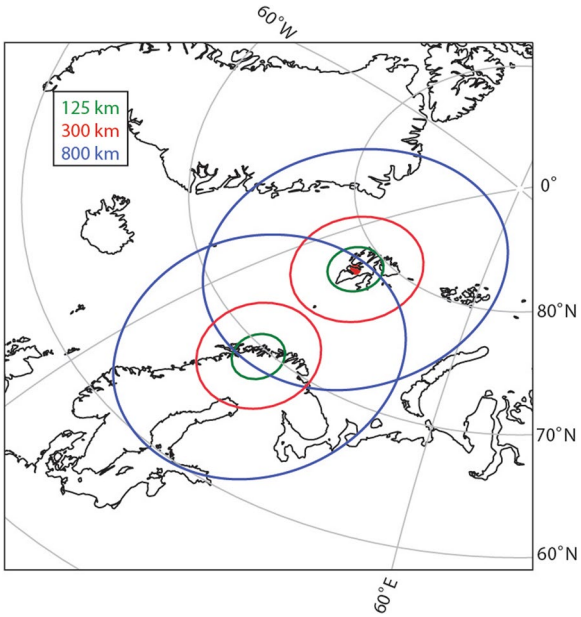

Fig. 3 Modelled fields-of-view (fovs) for both the new EISCAT_3D system (located in Mainland Northern Norway) and a new ISR system on Svalbard. A 30° elevation cut off and a vertical boresite is used for both fovs. The colour codes indicate the fov at the different altitudes, as indicated in the legend

A permanent optical station has been in place in Longyearbyen since 1978; first in the Adventdalen valley, and since 2008 on the Breinosa mountain as the Kjell Henriksen Observatory (KHO 2022), the largest optical observatory for auroral studies in the world. Optical instrumentation now exists at all four main settlements of Svalbard (Longyearbyen, Ny-Ålesund, Barentsburg and Hornsund). In addition, Svalbard is hosting multiple GNSS receivers, HF transmitters, ionosondes, dynasondes, riometers, ground magnetometers, an atmospheric MST radar (SOUSY), and an additional upper atmospheric HF radar (SuperDARN, Chisham et al. 2007). The ionosphere above Svalbard also benefits from being inside the field-of-view of two additional SuperDARN radars located in Finland and Iceland. The ESR is co-located with several of these facilities on the Breinosa mountain. Scientists from over 15 (as of 2022)

countries have instrumentation in the area dedicated to studies of the MLTI system.

Andøya Space Center (ASC 2022) operates two sounding rocket launch sites: one in Andøya (northern mainland Norway) and one in Ny-Ålesund (Svalrak). Both sites are capable of launching scientific payloads into the MLTI region above and around Svalbard.

The Svalbard archipelago is home to a vast research network of monitoring stations covering diverse topics such as biology, geology, glaciology, meteorology, oceanography, technology, and science tourism, in addition to the instrumentation located in the 4 main settlements mentioned above.

The University Centre in Svalbard (UNIS 2022) in Longyearbyen is the world's northernmost higher education institution. UNIS provides research-based education for the next generation of Arctic experts in biology, geology, geophysics and technology. The Arctic Geophysics Department owns and operates KHO, the Svalbard SuperDARN radar, as well as other smaller instrumentation. UNIS offers courses to Bachelor/Masters/PhD students from across the world with a dedicated hands-on (or field) experience. For the MLTI courses this involves fieldwork at the ESR and KHO. Educating the next generation of scientists and providing them with hands-on experience and skills is of critical importance. Cross-disciplinary research is necessary to obtain a complete understanding of the coupled Earth system. Recent work has highlighted the effects of the solar wind and the IMF on tropospheric pressure and temperatures (below 10 km height) (e.g. Lam et al. 2014; Burns et al. 2007).

Support for research is also given through Svalbard Integrated Earth Observing System (SIOS 2022) and Svalbard Science Forum (SSF 2022). In addition, Svalbard hosts the only commercial satellite ground station in the world that is capable of fully supporting all upload/download telemetry needs of a polar orbiting satellite (14 out of 14 orbits per day). The satellite station is operated by Kongsberg Satellite Services (KSAT 2022), and it is the largest in the world with more than 100 telemetry antennas. It supports several satellite missions including the ESA Landsat and Sentinel missions and the NASA NiSAR and PACE missions.

Both Longyearbyen and Ny-Ålesund (about 120 km further north) have high-speed (Gb) internet connection via optical fibre. This allows high-speed download, remote monitoring, and operation of scientific equipment. Longyearbyen is a thriving community with a dedicated power station and serves as an air and sea transport hub for equipment and people to the Norwegian mainland. The combination of research infrastructure, commercial investment, and community support is unique for a high Arctic region (at nearly 80°N). Historically, coal mining was the main industry on Svalbard, but this era is soon coming to an end. Currently, Norway has only one single mine in operation (Mine 7 at Breinosa), which is due to cease operations in 2025. Longyearbyen, and Svalbard as a whole, is now prioritizing further scientific research into renewable energy and climate change, with science tourism and satellite upload/download capabilities as the main areas for financial development. It is thus an ideal time to develop the next generation of ISR on Svalbard.

2.9 Location and radar design

Whilst the specific location for such a facility is not the main subject for this report, various design possibilities and considerations (logistical as well as scientific) will be briefly presented here. The current ESR is located about 20 km outside Longyearbyen, on the mountain Breinosa. It consists of two cassegrain dishes (one 42 m in diameter that is fixed parallel to the magnetic field lines, one 32 m in diameter that is fully steerable). The system is fed by a single transmitter system consisting of 16 klystrons. The site is connected to an optical network fibre and main power, with a backup battery bank in case of power cuts to maintain emergency heating, lighting and computer functions (but not to power the transmitters). There is a road to the site, which must be cleared from snow regularly over the winter season. It is currently maintained jointly by the local coal mining company and EISCAT. It is currently unclear how road access to Breinosa will be after closing of the coal mine (Mine 7) in 2025. One issue with the current site is backscatter from the nearby fjords (sea-clutter) in the side lobes. Due to its dynamic nature, it is not something that can be easily filtered out by the analysis software (unlike a mountain, which is generally less dynamic). As a consequence, it has limitations for the ability to monitor the lower parts of the MLTI system. For a new site location closer to Longyearbyen, it should be noted that there is an ongoing hearing (as of 2022) in regard to designating the land near Longyearbyen (lower Adventdalen) as a protected environmental area (Govenor of Svalbard (Sysselmesteren 2022). These highlighted issues must be taken into account when the location for the new facility is decided.

A new system will be of a phased array design for reasons highlighted earlier; the advanced technology allows near instantaneous monitoring of multiple directions simultaneously, with no moving parts, and not reliant on a small number of transmitter units (reducing risks of a single point of failure). This technology has been proven very successful in high Arctic conditions (RISR-N, RISR-C, PFISR). RISR-N and RISR-C rely on diesel generators for power, whilst PFISR has mains power. Various ISRs use different operating

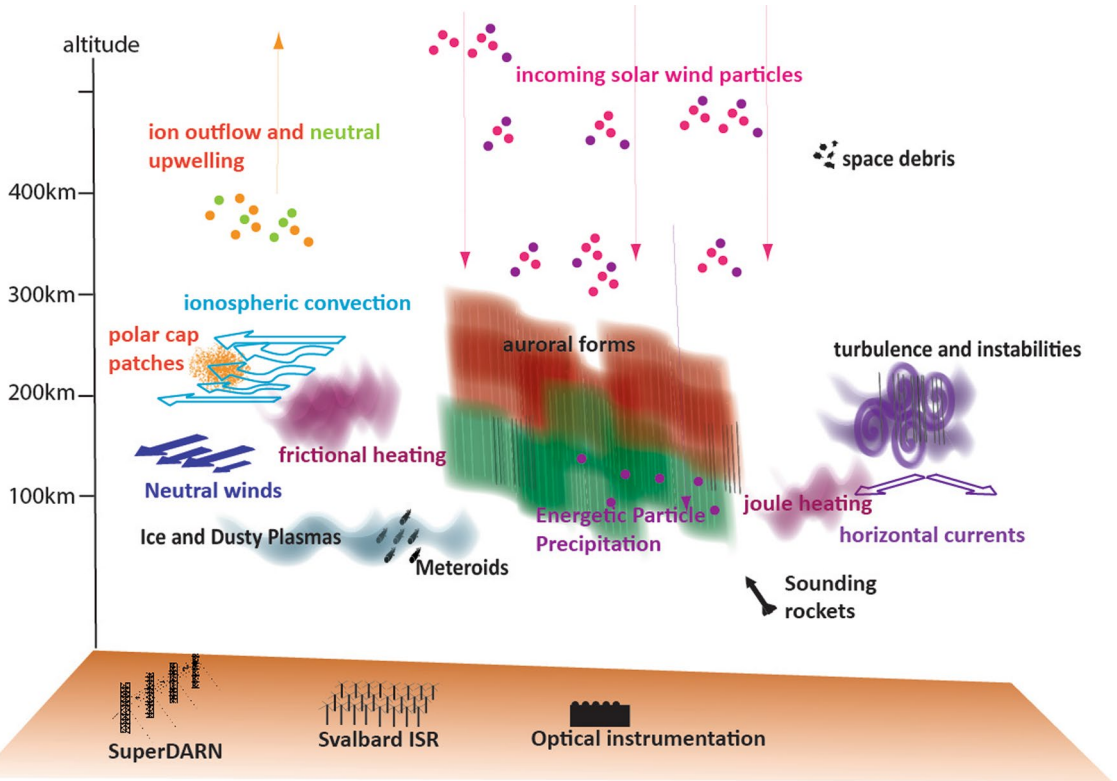

Fig. 4 Schematic showing the different MLTI phenomena described in the paper. The large scale infrastructure on Svalbard (optics, SuperDARN and the proposed ISR) are also shown

frequencies. The current ESR has an operating frequency of 500 MHz. PFISR operates at 449 MHz, RISR at 442 MHz, and the new EISCAT_3D system will operate at 223 MHz. The frequency, and thus wavelength, λ, of the transmitted signal has direct implications for the design of the transmitters and also the scale sizes of the targets it can observe.

An ISR is designed to maximize the received signal power which is based on a variety of parameters (some controlled from a design point of view, and some controlled by the nature of the target and the distance to it). The generalized for m of the radar equation, in the case of a homogenous beam filling target of volume V_s, relevant for ISR (e.g. Farley 1996; Bowles et al. 1962) is:

$$P_r = \frac{P_t G_t A_e}{(4\pi)^2 R_t^2 R_r^2} \int_{V_s} \sigma_r dV_s \tag{1}$$

where P_r is the received power, P_t is the transmitter power, G_t is the transmitter antenna gain, A_e is the effective area of the receiving antenna. The latter two terms (G_t and A_e) are also dependant on radar wavelength, λ. R_t is the distance from the transmitter to the target, R_r is the distance from the target to the receiver and σ_r is the radar scattering cross section of the target. From this equation it can be seen that, unsurprisingly, by increasing the transmitted power, the received power is also increased. However, the received power can also be increased/decreased by varying the size of the antenna field itself A_e, and the operating wavelength λ. This allows some degree of flexibility when considering the size of the antenna field and the power source.

The spatial extent and shape of an ISR beam is determined by its radiation pattern. This, in turn, is determined by a number of design factors related to, amongst other things, the size and number of the antenna elements and the relative distance between them. The main pointing direction (or boresite) also influences the shape of the radiation pattern. For the EISCAT_3D system the main site will have a near vertical boresite (elevation angle $\sim 90°$). The AMISRs (which are mounted on a large panel system that is titled relative to the ground), have a boresite with elevation angles of $\sim 74°$(PFISR) and $\sim 55°$(RISR). The advantage of a smaller elevation angle is that the total radar field of view (the furthest extent in azimuth and elevation that the radar beams can be electronically steered to) can be tilted and extended towards a particular latitude and longitude direction. The caveat is the limitation it

introduces for the location of the radar, requiring no substantial objects (e.g. mountains) in their immediate vicinity. A phased array design could also include an electromagnetic fence to mitigate unwanted scatter from non-atmospheric objects (such as the aforementioned sea-clutter). These facts should all be considered when a location for the system is decided. The flexibility of a new phased array system, in terms of number of beams, pointing directions and range resolution (operating modes), is one of its great benefits. Although the beam steering is now electronic (and thus can be done at the sub millisecond rate) there is still a trade-off to be negotiated between the spatial and temporal coverage. The signal-to-noise ratio on any particular beam (determined by the dwell time) must be sufficient to allow meaningful ionospheric parameters to be derived (i.e. with acceptable variances). Additionally, the range resolution (along the beam) is determined by the pulse length whilst the horizontal resolution is determined by the angular beam width and the operating frequency (all factors still to be determined for the new system). As a comparison, although the operating mode choices can be almost endless, the AMISRs tend to focus around some specific modes, dependent on the phenomena under observation. Gillies et al. (2016) used an 11 beam scan at 1 min resolution, with the beams separated such that it produced a 'scan' with a horizontal resolution of 0.25° magnetic latitude. Bahcivan et al. (2010) used a similar scan with a long pulse experiment resulting in 72 km range resolution. Dahlgren et al. (2012) extended the field of view using 25 beams in a 5 x 5 grid formation with a 1 min resolution. The grid had a horizontal extent of 300 x 400 km at F-region heights (300 km). One of the highest spatial and temporal resolution modes was documented by Semeter et al. (2009). The authors used a mode giving an 11 x 11 grid with a 14.6 s resolution. The grid had a horizontal extent of 65 x 60 km at E-region heights (100 km). The beams were 2 km wide with a 1.5 km range resolution. A new imaging technique called aperture synthesis radar imaging (ASRI) (e.g. Woodman 1997; Hysell and Chau 2012) could be applied to improve the horizontal resolution. This has been successfully implemented on other radar systems such as Jicamarca where the effective angular beam width was improved from $\sim 1°$(typical resolution for standard ISR system) to $\sim 0.1°$ (Chau and Woodman 2001). Modelling work by Stamm et al. (2021) has shown that ASRI could deliver an effective angular beam width of $\sim 0.05°$ resulting in a horizontal resolution of ~ 90 m at E-region altitude of 100 km using the EISCAT_3D core transmitter site only. Such a set up could be possible with the new Svalbard ISR. It is envisaged that the new ISR system will have similar, if not better, operating capabilities as the AMISRs (given the advance in technology since the AMISRs were built). The new ASRI technique also holds distinct promise. As such the new radar will vastly improve the ability to observe a variety of phenomena inside the polar cap and cusp at a far higher spatial and temporal resolution than is currently possible.

Whilst it is clear that the ISR must be of the phased array type, it is unclear whether a mono-static or bi-static configuration would be possible. The advantage with mono-static systems is that the transmitter and the receiver is co-located. In terms of operations this means that the microsecond timing required when transmitting and receiving the radar signal does not rely on a fast internet connection. The disadvantage is that, whilst full vector quantities can be obtained, they still require a beam swinging technique with some assumptions made about the ionosphere. A mono-static system, such as the AMISRs, would still be a vast improvement over the current system. Both RISR and PFISR have provided valuable new insight into polar cap phenomena in great detail (e.g. Dahlgren et al. 2014; Lyons et al. 2011; Gabrielse et al. 2018). In addition to the ASRI technique, a co-located interferometer array could also add additional functionality, providing additional possibilities for data with a sub-beam horizontal resolution (Grydeland et al. 2005). The ideal location for the transmitter would be in the vicinity of the main settlement of Longyearbyen, with access to mains power, network, and transport links. Since the power requirements for reception is several orders of magnitude less than that of the transmitter, then proximity to a large power supply is not crucial for the receiver system. Consequently, a possible location for a remote receiver system may be Ny-Ålesund, with its high speed network capability.

An example field of view of a phased array radar located near Longyearbyen is shown in Fig. 3. A 30 ° elevation cut off and a vertical boresite is used for the figure. The field of view of the new EISCAT_3D radar is also shown for context. The three coloured contours show the field of view of each radar at 125 km (green), 300 km (red), and 800 km (blue). As mentioned earlier, the field of view of the new EISCAT_3D site will not reach up to the cusp and polar cap at ionospheric altitudes. The figure illustrates how a near continuous field of view at ionospheric altitudes would be possible when EISCAT_3D is combined with a new Svalbard ISR. The two fields of view (at 300 km altitude) are also superimposed onto Fig. 2 (at 4 different MLTs showing how the combination of these systems would allow tracking of MLTI features into the dayside cusp and polar cap, and then out of the nightside polar cap and into the nightside auroral oval. As stated earlier in the paper, it is envisaged that the radar

is coming towards its end-of-life within the next 10 years. A prudent timeline, for the user community to work to would thus be to look towards having initial funding in place for a design study within the next 5 years, with the aim for a new radar system to be in place (either fully operational or have entered the building stage) within the next 10 years.

2.10 Importance of a cusp ISR for satellite and rocket missions

The benefits of coordinated observations in both ground and space are well demonstrated across the research community. These have ranged from single spacecraft missions (e.g. CHAMP, IMAGE, POLAR), via multiple spacecraft flying in close formation (SWARM, CLUSTER, MMS), to satellite networks (e.g. DMSP, IRIDIUM, POES). Spacecraft provide in situ observations of the drivers or energy sources of the system through measurements of plasma and magnetic field parameters, dynamical processes, and boundary locations in the solar wind, magnetosphere, and topside ionosphere. Space-based imagers can provide optical observations at multiple wavelengths of various auroral features (e.g. IMAGE, POLAR, DMSP, Reimei). Ground-based observations reveal both the energy sink inside the Earth's MLTI system (e.g. auroral features, turbulence, convection) and also the drivers of processes which feed energy and mass back into the magnetosphere (e.g. ion and neutral outflow) as is detailed in the previous sections.

Several new space missions will soon target the cusp and polar cap ionosphere with innovative instrumentation far beyond the state-of-the-art. At least four missions have strong links to Norway, with co-investigators from multiple universities and/or strong scientific interest. Close conjunctions with the current ESR, and the adjacent facilities in Svalbard, play a key role for a new era of ground-breaking MLTI science:

1. The Electrojet Zeeman Imaging Explorer (EZIE 2022) are three small satellites that will obtain magnetic field measurements at 80 km altitude of the auroral electrojet via remote sensing using the Zeeman effect. EZIE is a NASA mission to launch in 2024.
2. The Tandem Reconnection and Cusp Electrodynamics Reconnaissance Satellites (TRACERS 2022) are two identical satellites that will target spatial/temporal variation the Earth's cusps with a separation of only 10 s to 120 s. TRACERS is a NASA mission to launch in 2024.
3. The Lunar Environment Heliospheric X-ray Imager (LEXI 2022) will take global soft X-ray images from the lunar surface of the interaction of the solar wind and the Earth's magnetic field. LEXI is a NASA mission to launch in 2024.
4. The Solar wind Magnetosphere Ionosphere Link Explorer (SMILE) (Branduardi-Raymont et al. 2018) will obtain soft X-ray images of solar wind plasma entry at the magnetopause and into the cusps, and UV images of the Northern Hemispheric auroral oval. SMILE is a joint mission between ESA and the Chinese Academy of Science to launch in 2025.

In addition, the ground-based facilities at Svalbard have played a prominent role in several mission concepts like the NASA Meme-X (Moore et al. 2016) and the ESA ESCAPE proposal (Dandouras et al. 2017).

Sounding rockets provide the only means by which 'in situ' observations of the MLTI system is possible. The altitudes of interest are generally too high for high altitude balloons (which are limited to below about 30 km) and not feasible to maintain with a low altitude spacecraft (due to satellite drag). As mentioned in Sect. 2.8, Andoya Space Center, operates two sounding rocket launch sites both able to launch rockets into the cusp region above or around Svalbard. The recent Grand Challenge CUSP (CGI-CUSP) project in 2018–2021 (Blix et al. 2019), involved 12 sounding rockets funded by the space agencies of USA, Japan, and Norway. The current ESR has provided ground support to many rocket missions, e.g. SERSIO (Lorentzen et al. 2007), CUSP (Burchill et al. 2010), ICI-2 (e.g. Lorentzen et al. 2010; Moen et al. 2012; Oksavik et al. 2012), ICI-3 (Spicher et al. 2015), RENU2 (Lessard et al. 2020), SCIFER-2 (Lund et al. 2012) and CAPER2 (Moser et al. 2020). For each rocket mission the ESR is providing both real-time monitoring of the MLTI system (crucial for launch decisions) and larger scale context observations of the MLTI system throughout the rocket flight. The ESR data sets are vital in allowing the detailed (very high temporal and spatial resolution) rocket observations to be understood and related to the dynamics of the larger scale turbulence and processes within the MLTI system, prior to, after and during the rocket flight time. The upcoming CGI-MLT (mesosphere lower thermosphere) project, 2022–2026) (Grand Challenge 2022) will also play an important role in understanding the vertical coupling of atmospheric layers in the MLTI system. This combination of available ground-, space- and rocket-based instrumentation is unique in the world and means the required cross scale, 3D approach can be taken, as highlighted by the review papers in Sect. 1.

3 Conclusions

The current ESR has provided an unprecedented dataset of parameters needed to characterize the MLTI region over Svalbard, inside the cusp and polar cap regions. This paper has summarized some of the main research topics along with examples of how the data from the ESR has proved vital in increasing our understanding on how energy, mass and momentum is transferred and dissipated into the MLTI system. The paper has also provided examples of unanswered scientific questions within the research field and provided a compelling argument as to how a new phased array ISR on Svalbard would address these questions. This paper discusses how Svalbard remains unique in the world in terms of its ability to monitor the cusp region with multiple ground- and rocket-based instruments. It has excellent support infrastructure, both in terms of logistics and educational opportunities for the next generation of scientists and engineers. The new radar is also in a unique position in its ability to provide data and monitoring in two relatively new areas of societal concern—space debris and space weather events. With its volumetric imaging across various spatial and temporal scales a new ISR would provide the required data sets discussed and highlighted as a priority in the recent review papers (e.g. Sarris 2019; Palmroth et al. 2021; Heelis and Maute 2020). The location of the radar and the proposed field of view will also complement the new EISCAT_3D system on the mainland, allowing a near continuous coverage of the auroral, cusp and polar cap regions from 65° to 82° latitude. A new Svalbard ISR system should thus be a priority for the scientific community.

Abbreviations

EISCAT	European Incoherent Scatter Scientific Association
PFISR	Poke flat incoherent scatter radar
RISR	Resolute bay incoherent scatter radar
IPY	International polar year
MLTI	Mesosphere/lower thermosphere/ionosphere system
ESA	European Space Agency
ESR	EISCAT Svalbard radar
EZIE	Electrojet Zeeman Imaging Explorer
LEXI	Lunar Environment Heliospheric X-ray Image
NASA	National Aeronautics and Space Administration
SMILE	Solar wind Magnetosphere Ionosphere Link Explorer
TRACERS	Tandem Reconnection and Cusp Electrodynamics Reconnaissance Satellites

Acknowledgements

LB acknowledges helpful discussions with R. Varney (UCLA) and C. Heinselman (EISCAT director) in the writing of this manuscript. We acknowledge the Community Coordinated Modeling Center (CCMC) at Goddard Space Flight Center for the use of the IRI-16 and NRL-MSIS 2.0 models https://ccmc.gsfc.nasa.gov/models/IRI~2016/https://ccmc.gsfc.nasa.gov/models/NRLMSIS~v2.0.

Author contributions

LB proposed the topic, organized the paper and assigned tasks to the co-authors. Individual co-authors took a lead on writing the different sections of the paper. All authors read and approved the final manuscript.

Funding

This work was funded through Norwegian Research Council Grant: 329681.

Availability of data and materials

Not applicable.

Declarations

Competing interests

The authors declare that they have no competing interest.

Author details

[1]University Centre in Svalbard, Postboks 156, Longyearbyen, Svalbard 9171, Norway. [2]UiT The Arctic University of Norway, Tromsø, Norway. [3]Department of Physics and Technology, Birkeland Centre for Space Science, University of Bergen, Allégaten 55, Bergen 5020, Norway. [4]University of Oslo, Oslo, Norway.

Received: 2 November 2022 Accepted: 20 August 2023
Published online: 04 September 2023

References

Aikio AT, Lakkala T, Kozlovsky A, Williams PJS (2002) Electric fields and currents of stable drifting auroral arcs in the evening sector. J Geophys Res Space Phys 107(A12):3–1314. https://doi.org/10.1029/2001JA009172

Andersson ME, Verronen PT, Rodger CJ, Clilverd MA, Seppälä A (2014) Missing driver in the Sun-Earth connection from energetic electron precipitation impacts mesospheric ozone. Nat Commun 5:5197

André M, Eriksson AI, Khotyaintsev YV, Toledo-Redondo S (2021) The spacecraft wake: interference with electric field observations and a possibility to detect cold ions. J Geophys Res Space Phys 126(9):29493. https://doi.org/10.1029/2021JA029493

ASC homepage. Accessed 13 Oct 2022. https://www.andoyaspace.no/

Baddeley L, Yeoman T, Wright D, Trattner K, Kellet B (2005) On the coupling between unstable magnetospheric particle populations and resonant high m ulf wave signatures in the ionosphere, vol 23(2). Copernicus GmbH, pp 567–577

Baddeley LJ, Lorentzen DA, Partamies N, Denig M, Pilipenko V, Oksavik K, Chen X, Zhang Y (2017) Equatorward propagating auroral arcs driven by ulf wave activity: multipoint ground-and space-based observations in the dusk sector auroral oval. J Geophys Res Space Phys 122(5):5591–5605

Bahcivan H, Tsunoda R, Nicolls M, Heinselman C (2010) Initial ionospheric observations made by the new resolute incoherent scatter radar and comparison to solar wind imf. Geophys Res Lett. https://doi.org/10.1029/2010GL043632

Basu S, MacKenzie E, Basu S (1988a) Ionospheric constraints on vhf/uhf communications links during solar maximum and minimum periods. Radio Sci 23(03):363–378

Basu S, Basu S, MacKenzie E, Fougere PF, Coley WR, Maynard NC, Winningham JD, Sugiura M, Hanson WB, Hoegy WR (1988b) Simultaneous density and electric field fluctuation spectra associated with velocity shears in the auroral oval. J Geophys Res Space Phys 93(A1):115–136. https://doi.org/10.1029/JA093iA01p00115

Baumann, C, Rapp, M, Kero, A, Enell, C-F (2013) Meteor smoke influences on the d-region charge balance–review of recent in situ measurements and one-dimensional model results. In: Annales Geophysicae, vol 31. Copernicus GmbH, pp 2049–2062

Baumann C, Rapp M, Kero A (2016) Secondary electron emission from meteoric smoke particles inside the polar ionosphere. Annales Geophysicae 34(6):573–580

Baumjohann W, Treumann RA (1997) Advanced space plasma physics. World Scientific

Bilitza D, Altadill D, Truhlik V, Shubin V, Galkin I, Reinisch B, Huang X (2017) International reference ionosphere 2016: from ionospheric climate to real-time weather predictions. Space Weather 15(2):418–429. https://doi.org/10.1002/2016SW001593

Billett D, Hosokawa K, Grocott A, Wild J, Aruliah A, Ogawa Y, Taguchi S, Lester M (2020) Multi-instrument observations of ion-neutral coupling in the dayside cusp. Geophys Res Lett 47(4):2019–085590

Bjoland LM, Ogawa Y, Løvhaug UP, Lorentzen DA, Hatch SM, Oksavik K (2021) Electron density depletion region observed in the polar cap ionosphere. J Geophys Res Space Phys 126(1):28432. https://doi.org/10.1029/2020JA028432

Bland EC, Heino E, Kosch MJ, Partamies N (2018) Superdarn radar-derived hf radio attenuation during the September 2017 solar proton events. Space Weather 16(10):1455–1469

Blix K, Rowland DE, Kletzing C, Labelle JW, Moen J, Koehler C (2019) Grand challenge initiative-cusp and m/lt projects. In: AGU fall meeting abstracts, vol 2019, pp 34–01. https://www.grandchallenge.no/project-cusp/

Bowles KL, Ochs G, Green J (1962) On the absolute intensity of incoherent scatter echoes from the ionosphere. J Res NBS D 66:395–407

Branduardi-Raymont G, Wang C, Escoubet CP, Adamovic M, Agnolon D, Berthomier M, Carter JA, Chen W, Colangeli L, Collier M, Connor HK, Dai L, Dimmock A, Djazovski O, Donovan E, Eastwood JP, Enno G, Giannini F, Huang L, Kataria D, Kuntz K, Laakso H, Li J, Li L, Lui T, Loicq J, Masson A, Manuel J, Parmar A, Piekutowski T, Read AM, Samsonov A, Sembay S, Raab W, Ruciman C, Shi JK, Sibeck DG, Spanswick EL, Sun T, Symonds K, Tong J, Walsh B, Wei F, Zhao D, Zheng J, Zhu X, Zhao Z (2018) Smile definition study report, vol 1, pp 1–86

Burchill J, Knudsen D, Clemmons J, Oksavik K, Pfaff R, Steigies C, Yau A, Yeoman TK (2010) Thermal ion upflow in the cusp ionosphere and its dependence on soft electron energy flux. J Geophys Res Space Phys 115(A5):66

Burns G, Tinsley B, Frank-Kamenetsky A, Bering E (2007) Interplanetary magnetic field and atmospheric electric circuit influences on ground-level pressure at vostok. J Geophys Res Atmos 112(D4):66

Burston R, Mitchell C, Astin I (2016) Polar cap plasma patch primary linear instability growth rates compared. J Geophys Res Space Phys 121(4):3439–3451. https://doi.org/10.1002/2015JA021895

Cai L, Aikio A, Milan S (2016) Joule heating hot spot at high latitudes in the afternoon sector. J Geophys Res Space Phys 121(7):7135–7152

Carlson HC (2012) Sharpening our thinking about polar cap ionospheric patch morphology, research, and mitigation techniques. Radio Sci 47(4):66. https://doi.org/10.1029/2011RS004946

Carlson HC, Oksavik K, Moen J, van Eyken AP, Guio P (2002) Esr mapping of polar-cap patches in the dark cusp. Geophys Res Lett 29(10):24–1244. https://doi.org/10.1029/2001GL014087

Carlson HC Jr, Oksavik K, Moen J, Pedersen T (2004) Ionospheric patch formation: direct measurements of the origin of a polar cap patch. Geophys Res Lett 31(8):66. https://doi.org/10.1029/2003GL018166

Carlson HC, Pedersen T, Basu S, Keskinen M, Moen J (2007) Case for a new process, not mechanism, for cusp irregularity production. J Geophys Res Space Phys 112(A11):66. https://doi.org/10.1029/2007JA012384

Chandler MO, Waite JH, Moore TE (1991) Observations of polar ion outflows. J Geophys Res Space Phys 96(A2):1421–1428. https://doi.org/10.1029/90JA02180

Chau JL, Woodman RF (2001) Three-dimensional coherent radar imaging at Jicamarca: comparison of different inversion techniques. J Atmos Solar-Terr Phys 63(2–3):253–261

Chisham G, Lester M, Milan S, Freeman M, Bristow W, Grocott A, McWilliams K, Ruohoniemi J, Yeoman T, Dyson PL et al (2007) A decade of the super dual auroral radar network (superdarn): scientific achievements, new techniques and future directions. Surv Geophys 28(1):33–109

Cladis JB, Collin HL, Lennartsson OW, Moore TE, Peterson WK, Russell CT (2000) Observations of centrifugal acceleration during compression of magnetosphere. Geophys Res Lett 27(7):915–918. https://doi.org/10.1029/1999GL010737

Collis PN (1996) The high latitude d-region and mesosphere revealed by the eiscat incoherent scatter radars during solar proton events. Adv Space Res 18(3):83–92

Collis PN, Rietveld MT (1990) Mesospheric observations with the EISCAT UHF radar during polar cap absorption events: 1. Electron densities and negative ions. Annales Geophysicae 8:809–824

Comfort RH (1988) The magnetic mirror force in plasma fluid models. Model Magnetos Plasma 44:51–53

Cresswell-Moorcock K, Rodger CJ, Kero A, Collier AB, Clilverd MA, Häggström I, Pitkänen T (2013) A reexamination of latitudinal limits of substorm-produced energetic electron precipitation. J Geophys Res Space Phys 118(10):6694–6705

Dahlgren H, Perry GW, Semeter JL, St.-Maurice J-P, Hosokawa K, Nicolls MJ, Greffen M, Shiokawa K, Heinselman C (2012) Space-time variability of polar cap patches: direct evidence for internal plasma structuring. J Geophys Res Space Phys. https://doi.org/10.1029/2012JA017961

Dahlgren H, Perry G, St Maurice J-P, Sundberg T, Hosokawa K, Semeter JL, Nicolls MJ, Shiokawa K (2014) 3d imaging reveals electrodynamics of polar cap aurora. Astron Geophys 55(5):5–26

Dandouras I (2021) Ion outflow and escape in the terrestrial magnetosphere: cluster advances. J Geophys Res Space Phys 126(10):2021–029753. https://doi.org/10.1029/2021JA029753

Dandouras I, Yamauchi M, Rème H, De Keyser J, Marghitu O, Fazakerley A, Grison B, Kistler L, Milillo A, Nakamura R, Paschalidis N, Paschalis A, Pinçon J-L, Sakanoi T, Wieser M, Wurz P, Yoshikawa I, Häggström I, Liemohn M, Tian F (2017) European SpaceCraft for the study of Atmospheric Particle Escape (ESCAPE): a mission proposed in response to the ESA M5-call. In: EGU General Assembly Conference Abstracts, vol 19, p 5456

David TW, Wright DM, Milan SE, Cowley SWH, Davies JA, McCrea I (2018) A study of observations of ionospheric upwelling made by the Eiscat Svalbard radar during the international polar year campaign of 2007. J Geophys Res Space Phys 123(3):2192–2203. https://doi.org/10.1002/2017JA024802

Deshpande KB, Zettergren MD (2019) Satellite-beacon ionospheric-scintillation global model of the upper atmosphere (sigma) iii: scintillation simulation using a physics-based plasma model. Geophys Res Lett 46(9):4564–4572. https://doi.org/10.1029/2019GL082576

Dyson PL, Winningham JD (1974) Top side ionospheric spread F and particle precipitation in the day side magnetospheric clefts. J Geophys Res 79(34):5219–5230. https://doi.org/10.1029/JA079i034p05219

EISCAT homepage. https://eiscat.se/eiscat3d-information/. Accessed 13 Oct 2022

Emmert JT, Drob DP, Picone JM, Siskind DE, Jones M Jr, Mlynczak MG, Bernath PF, Chu X, Doornbos E, Funke B, Goncharenko LP, Hervig ME, Schwartz MJ, Sheese PE, Vargas F, Williams BP, Yuan T (2021) Nrlmsis 2.0: a whole-atmosphere empirical model of temperature and neutral species densities. Earth Space Sci 8(3):2020. https://doi.org/10.1029/2020EA001321

Enengl F, Partamies N, Ivchenko N, Baddeley L (2021) On the relationship of energetic particle precipitation and mesopause temperature. Annales Geophysicae 39(5):795–809

EU Department of Defence Industry and Space (2021) Eu space program. https://ec.europa.eu/info/sites/default/files/about_the_european_commission/eu_budget/ps_db2023_space_h1_1.pdf, accessed 13 October 2022

EZIE (2022) homepage. https://www.jhuapl.edu/PressRelease/201229-NASA-selects-EZIE-heliophysics. Accessed 13 Oct 2022

Farley D (1996) Incoherent scatter radar probing. Modern ionospheric science. Katlenburg Lindau Copernicus GmbH, pp 415–439

Fasel GJ (1995) Dayside poleward moving auroral forms: a statistical study. J Geophys Res Space Phys 100(A7):11891–11905. https://doi.org/10.1029/95JA00854

Fear RC, Trenchi L, Coxon JC, Milan SE (2017) How much flux does a flux transfer event transfer? J Geophys Res Space Phys 122(12):12310–12327. https://doi.org/10.1002/2017JA024730

Fenrich FR, Gillies DM, Donovan E, Knudsen D (2019) Flow velocity and field-aligned current associated with field line resonance: Superdarn measurements. J Geophys Res Space Phys 124(6):4889–4904

Ferguson DC, Worden SP, Hastings DE (2015) The space weather threat to situational awareness, communications, and positioning systems. IEEE Trans Plasma Sci 43(9):3086–3098

Flegel S, Gelhaus J, Wiedemann C, Vorsmann P, Oswald M, Stabroth S, Klinkrad H, Krag H (2009) The master-2009 space debris environment model. Fifth European conference on space debris, vol 672. European Space Agency/European Space Operations Centre Darmstadt, Germany, pp 1–8

Forsythe VV, Makarevich RA (2018) Statistical analysis of the electron density gradients in the polar cap f region using the resolute bay incoherent scatter radar north. J Geophys Res Space Phys 123(5):4066–4079. https://doi.org/10.1029/2017JA025156

Frey HU, Han D, Kataoka R, Lessard MR, Milan SE, Nishimura Y, Strangeway RJ, Zou Y (2019) Dayside aurora. Space Sci Rev 215(8):1–32

Gabrielse C, Nishimura Y, Lyons L, Gallardo-Lacourt B, Deng Y, Donovan E (2018) Statistical properties of mesoscale plasma flows in the nightside high-latitude ionosphere. J Geophys Res Space Phys 123(8):6798–6820. https://doi.org/10.1029/2018JA025440
Ganguli G, Keskinen M, Romero H, Heelis R, Moore T, Pollock C (1994) Coupling of microprocesses and macroprocesses due to velocity shear: an application to the low-altitude ionosphere. J Geophys Res Space Phys 99(A5):8873–8889
Gao H, Shepherd GG, Tang Y, Bu L, Wang Z (2017) Double-layer structure in polar mesospheric clouds observed from sofie/aim, vol 35 (no 2). Copernicus GmbH, pp 295–309
Gary SP, Cole TE (1983) Pedersen density drift instabilities. J Geophys Res Space Phys 88(A12):10104–10110. https://doi.org/10.1029/JA088iA12p10104
Gillies RG, van Eyken A, Spanswick E, Nicolls M, Kelly J, Greffen M, Knudsen D, Connors M, Schutzer M, Valentic T, Malone M, Buonocore J, St.-Maurice J-P, Donovan E (2016) First observations from the risr-c incoherent scatter radar. Radio Sci 51(10):1645–1659. https://doi.org/10.1002/2016RS006062
Goertz C, Nielsen E, Korth A, Glassmeier KH, Haldoupis C, Hoeg P, Hayward D (1985) Observations of a possible ground signature of flux transfer events. J Geophys Res Space Phys 90(A5):4069–4078
Gondarenko NA, Guzdar PN (2004) Plasma patch structuring by the nonlinear evolution of the gradient drift instability in the high-latitude ionosphere. J Geophys Res Space Phys 109(A9):66. https://doi.org/10.1029/2004JA010504
Gordon WE (1958) Incoherent scattering of radio waves by free electrons with applications to space exploration by radar. Proc IRE 46(11):1824–1829
Govenor of Svalbard (Sysselmesteren) (2016) Risk and venerability analysis. https://www.sysselmesteren.no/contentassets/9fe94109ede443d89550f85263497240/ros-analyse-svalbard2.pdf. Accessed 13 Oct 2022
Govenor of Svalbard (Sysselmesteren) (2022) homepage. https://www.sysselmesteren.no/nb/om-sysselmesteren/miljovern/forvaltning-av-verneomrader/pagaende-forvaltningsplaner/verneforslag-for-nedre-adventdalen. Accessed 13 Oct 2022
Government of Canada (2021) Space weather canada. https://www.nrcan.gc.ca/science-and-data/science-and-research/natural-hazards/10657. Accessed 13 Oct 2022
Grand Challenge (2022) homepage. https://www.grandchallenge.no/project-mesosphere-lower- thermosphere/. Accessed 13 Oct 2022
Gray LJ, Beer J, Geller M, Haigh JD, Lockwood M, Matthes K, Cubasch U, Fleitmann D, Harrison G, Hood L, Luterbacher J, Meehl GA, Shindell D, van Geel B, White W (2010) Solar influences on the climate. Rev Geophys 48(4):66
Grydeland T, Chau JL, La Hoz C, Brekke A (2005) An imaging interferometry capability for the EISCAT Svalbard radar. Annales Geophysicae 23(1):221–230. https://doi.org/10.5194/angeo-23-221-2005
Gunnarsdottir TL, Mann I (2021) Charged dust in the d-region incoherent scatter spectrum. J Plasma Phys 87(5):66
Hargreaves JK, Ranta H, Ranta A, Turunen E, Turunen T (1987) Observations of the polar cap absorption event of February 1984 by the EISCAT incoherent scatter radar. Planet Space Sci 35(7):947–958
Hargreaves JK, Shirochkov AV, Farmer AD (1993) The polar cap absorption event of 19–21 March 1990: recombination coefficients, the twilight transition and the midday recovery. J Atmos Terr Phys 55(6):857–862
Heelis RA, Maute A (2020) Challenges to understanding the Earth's ionosphere and thermosphere. J Geophys Res Space Phys 125:66. https://doi.org/10.1029/2019JA027497
Heppner JP, Liebrecht MC, Maynard NC, Pfaff RF (1993) High-latitude distributions of plasma waves and spatial irregularities from DE 2 alternating current electric field observations. J Geophys Res Space Phys 98(A2):1629–1652. https://doi.org/10.1029/92JA01836
Herlingshaw K, Baddeley LJ, Oksavik K, Lorentzen DA (2020) A statistical study of polar cap flow channels and their imf by dependence. J Geophys Res Space Phys 125(11):2020–028359. https://doi.org/10.1029/2020JA028359
Hervig M, Thompson RE, McHugh M, Gordley LL, Russell JM III, Summers ME (2001) First confirmation that water ice is the primary component of polar mesospheric clouds. Geophys Res Lett 28(6):971–974. https://doi.org/10.1029/2000GL012104
Horstmann A, Manis A, Braun V, Matney M, Vavrin A, Gates D, Seago J, Anz-Meador P, Wiedemann C, Lemmens S (2021) Flux comparison of master-8 and ordem 3.1 modelled space debris population. In: 8th European conference on space debris, Darmstadt
Hosokawa K, Taguchi S, Ogawa Y, Aoki T (2012) Periodicities of polar cap patches. J Geophys Res Space Phys 118(1):447–453. https://doi.org/10.1029/2012JA018165
Hysell D, Chau JL (2012) Aperture synthesis radar imaging for upper atmospheric research. In: Bech J, Chau JL (eds) Doppler radar observations—weather radar, wind profiler, ionospheric radar, and other advanced applications. Chapters, IntechOpen. https://doi.org/10.5772/39024
Ivarsen MF, Jin Y, Spicher A, Clausen LBN (2019) Direct evidence for the dissipation of small-scale ionospheric plasma structures by a conductive e region. J Geophys Res Space Phys 124(4):2935–2942. https://doi.org/10.1029/2019JA026500
Jacobsen KS, Dähnn M (2014) Statistics of ionospheric disturbances and their correlation with gnss positioning errors at high latitudes. J Space Weather Space Clim 4:27
Jia J, Kero A, Kalakoski N, Szeląg ME, Verronen PT (2020) Is there a direct solar proton impact on lower-stratospheric ozone? Atmos Chem Phys 20:14969–14982
Jin Y, Moen JI, Miloch WJ (2015) On the collocation of the cusp aurora and the GPS phase scintillation: a statistical study. J Geophys Res Space Phys 120(10):9176–9191. https://doi.org/10.1002/2015JA021449
Jin Y, Spicher A, Xiong C, Clausen LBN, Kervalishvili G, Stolle C, Miloch WJ (2019a) Ionospheric plasma irregularities characterized by the swarm satellites: statistics at high latitudes. J Geophys Res Space Phys 124(2):1262–1282. https://doi.org/10.1029/2018JA026063
Jin Y, Xing Z, Zhang Q, Wang Y, Ma Y (2019a) Polar cap patches observed by the EISCAT svalbard radar: a statistical study of its dependence on the solar wind and imf conditions. J Atmos Solar Terr Phys 192:104768. https://doi.org/10.1016/j.jastp.2018.01.011
Kelley MC (2009) The Earth's ionosphere: plasma physics and electrodynamics. Elsevier, Amsterdam
Kelley MC, Vickrey JF, Carlson CW, Torbert R (1982) On the origin and spatial extent of high-latitude F region irregularities. J Geophys Res Space Phys 87(A6):4469–4475. https://doi.org/10.1029/JA087iA06p04469
Kero J, Campbell-Brown MD, Stober G, Chau JL, Mathews JD, Pellinen-Wannberg A (2019) Radar observations of meteors. In: Sources of meteors on earth and beyond, meteoroids, p 65
Kersley L, Pryse SE, Wheadon NS (1988) Small scale ionospheric irregularities near regions of soft particle precipitation: scintillation and EISCAT observations. J Atmos Terr Phys 50(12):1047–1055. https://doi.org/10.1016/0021-9169(88)90094-3
Kervalishvili G, Lühr H (2013) The relationship of thermospheric density anomaly with electron temperature, small-scale fac, and ion up-flow in the cusp region, as observed by champ and dmsp satellites. Annales Geophysicae 31(3):541–554
Kervalishvili GN, Lühr H (2018) Climatology of air upwelling and vertical plasma flow in the terrestrial cusp region: seasonal and imf-dependent processes. Magn Fields Solar Syst 66:293–329
Keskinen MJ, Ossakow SL (1983) Theories of high-latitude ionospheric irregularities: a review. Radio Sci 18(6):1077–1091. https://doi.org/10.1029/RS018i006p01077
Keskinen MJ, Mitchell HG, Fedder JA, Satyanarayana P, Zalesak ST, Huba JD (1988) Nonlinear evolution of the Kelvin–Helmholtz instability in the high-latitude ionosphere. J Geophys Res Space Phys 93(A1):137–152. https://doi.org/10.1029/JA093iA01p00137
Kessler DJ, Cour-Palais BG (1978) Collision frequency of artificial satellites: the creation of a debris belt. J Geophys Res Space Phys 83(A6):2637–2646
Kessler DJ, Johnson NL, Liou J, Matney M (2010) The Kessler syndrome: implications to future space operations. Adv Astronaut Sci 137(8):66
KHO (2022) homepage. http://kho.unis.no/. Accessed 13 Oct 2022
Kintner PM, Seyler CE (1985) The status of observations and theory of high latitude ionospheric and magnetospheric plasma turbulence. Space Sci Rev 41(1):91–129. https://doi.org/10.1007/BF00241347
Kintner PM, Ledvina BM, de Paula ER (2007) Gps and ionospheric scintillations. Space Weather 5(9):66. https://doi.org/10.1029/2006SW000260
Klinkrad H (2006) Space debris: models and risk analysis. Springer, Berlin
Kosch M, Yiu I, Anderson C, Tsuda T, Ogawa Y, Nozawa S, Aruliah A, Howells V, Baddeley L, McCrea I et al (2011) Mesoscale observations of joule heating near an auroral arc and ion-neutral collision frequency in the polar cap e region. J Geophys Res Space Phys 116(A5):66

Krisko, P.H (2014) The new NASA orbital debris engineering model ordem 3.0. In: AIAA/AAS Astrodynamics Specialist Conference, p 4227
KSAT (2022) homepage. https://www.kongsberg.com/kda/what-we-do/space/products/satellite-services/. Accessed 13 Oct 2022
Lam MM, Chisham G, Freeman MP (2014) Solar wind-driven geopotential height anomalies originate in the Antarctic lower troposphere. Geophys Res Lett 41(18):6509–6514
Lamarche LJ, Makarevich RA (2017) Radar observations of density gradients, electric fields, and plasma irregularities near polar cap patches in the context of the gradient-drift instability. J Geophys Res Space Phys 122(3):3721–3736. https://doi.org/10.1002/2016JA023702
Lamarche LJ, Varney RH, Siefring CL (2020) Analysis of plasma irregularities on a range of scintillation-scales using the resolute bay incoherent scatter radars. J Geophys Res Space Phys 125(3):2019–027112. https://doi.org/10.1029/2019JA027112
Lamarche LJ, Deshpande KB, Zettergren MD (2022) Observations and modeling of scintillation in the vicinity of a polar cap patch. J Space Weather Space Clim 12:27. https://doi.org/10.1051/swsc/2022023
Latteck R, Strelnikova I (2015) Extended observations of polar mesosphere winter echoes over andøya (69 n) using Maarsy. J Geophys Res Atmos 120(16):8216–8226
Lessard MR, Fritz B, Sadler B, Cohen I, Kenward D, Godbole N, Clemmons JH, Hecht JH, Lynch KA, Harrington M, Roberts TM, Hysell D, Crowley G, Sigernes F, Syrjäsuo M, Ellingsen P, Partamies N, Moen J, Clausen L, Oksavik K, Yeoman T (2020) Overview of the rocket experiment for neutral upwelling sounding rocket 2 (renu2). Geophys Res Lett 47(21):2018–081885. https://doi.org/10.1029/2018GL081885
LEXI (2022) homepage. https://sites.bu.edu/lexi/. Accessed 13 Oct 2022
Linson LM, Workman JB (1970) Formation of striations in ionospheric plasma clouds. J Geophys Res 75(16):3211–3219. https://doi.org/10.1029/JA075i016p03211
Lockwood M, McWilliams KA (2021) A survey of 25 years' transpolar voltage data from the superdarn radar network and the expanding-contracting polar cap model. J Geophys Res Space Phys 126(9):2021–029554. https://doi.org/10.1029/2021JA029554
Lockwood M, Davies J, Moen J, Van Eyken A, Oksavik K, McCrea I, Lester M (2005) Motion of the dayside polar cap boundary during substorm cycles: Ii. generation of poleward-moving events and polar cap patches by pulses in the magnetopause reconnection rate. Annales Geophysicae 23(11):3513–3532
Lorentzen D, Kintner P, Moen J, Sigernes F, Oksavik K, Ogawa Y, Holmes J (2007) Pulsating dayside aurora in relation to ion upflow events during a northward interplanetary magnetic field (imf) dominated by a strongly negative imf by. J Geophys Res Space Phys 112(A3):66
Lorentzen DA, Moen J, Oksavik K, Sigernes F, Saito Y, Johnsen MG (2010) In situ measurement of a newly created polar cap patch. J Geophys Res Space Phys 115(A12):66. https://doi.org/10.1029/2010JA015710
Lühr H, Rother M, Köhler W, Grunwaldt L (2004) Thermospheric up-welling in the cusp region: evidence from champ observations. Geophys Res Lett 31(6):66. https://doi.org/10.1029/2003GL019314
Lund E, Lessard M, Sigernes F, Lorentzen D, Oksavik K, Kintner P, Lynch K, Huang D, Zhang B, Yang H et al (2012) Electron temperature in the cusp as measured with the scifer-2 sounding rocket. J Geophys Res Space Phys 117(A6):66
Lyons LR, Nishimura Y, Kim H-J, Donovan E, Angelopoulos V, Sofko G, Nicolls M, Heinselman C, Ruohoniemi JM, Nishitani N (2011) Possible connection of polar cap flows to pre- and post-substorm onset pbis and streamers. J Geophys Res Space Phys 116(A12):66. https://doi.org/10.1029/2011JA016850
Lyons LR, Nishimura Y, Zou Y (2016) Unsolved problems: mesoscale polar cap flow channels' structure, propagation, and effects on space weather disturbances. J Geophys Res Space Phys 121(4):3347–3352. https://doi.org/10.1002/2016JA022437
Maeda S, Nozawa S, Ogawa Y, Fujiwara H (2005) Comparative study of the high-latitude E region ion and neutral temperatures in the polar cap and the auroral region derived from the EISCAT radar observations. J Geophys Res Space Phys 110(A8):08301. https://doi.org/10.1029/2004JA010893
Maes L, Maggiolo R, De Keyser J, Dandouras I, Fear RC, Fontaine D, Haaland S (2015) Solar illumination control of ionospheric outflow above polar cap arcs. Geophys Res Lett 42:1304–1311. https://doi.org/10.1002/2014GL062972
Mager P, Klimushkin DY (2008) Alfvén ship waves: high-m ulf pulsations in the magnetosphere generated by a moving plasma inhomogeneity. Annales Geophysicae 26(6):1653–1663
Makarevich RA (2016) Toward an integrated view of ionospheric plasma instabilities: 2. Three inertial modes of a cubic dispersion relation. J Geophys Res Space Phys 121(7):6855–6869. https://doi.org/10.1002/2016JA022864
Makarevich RA, Crowley G, Azeem I, Ngwira C, Forsythe VV (2021) Auroral e-region as a source region for ionospheric scintillation. J Geophys Res Space Phys 126(5):2021–029212. https://doi.org/10.1029/2021JA029212
Maliniemi V, Marsh R Daniel, Tyssøy HN, Smith-Johnsen C (2020) Will climate change impact polar nox produced by energetic particle precipitation? Geophys Res Lett 47(9):2020–087041
Markkanen J, Jehn R, Krag H (2009) Eiscat space debris during the ipy-a 5000 hour campaign. In: Proceedings of the 5th ESA space debris conference, vol 625
McCrea I, Aikio A, Alfonsi L, Belova E, Buchert S, Clilverd M, Engler N, Gustavsson B, Heinselman C, Kero J et al (2015) The science case for the eiscat_3d radar. Prog Earth Planet Sci 2(1):1–63
Mevius M, van der Tol S, Pandey VN, Vedantham HK, Brentjens MA, de Bruyn AG, Abdalla FB, Asad KMB, Bregman JD, Brouw WN, Bus S, Chapman E, Ciardi B, Fernandez ER, Ghosh A, Harker G, Iliev IT, Jelić V, Kazemi S, Koopmans LVE, Noordam JE, Offringa AR, Patil AH, van Weeren RJ, Wijnholds S, Yatawatta S, Zaroubi S (2016) Probing ionospheric structures using the Lofar radio telescope. Radio Sci 51(7):927–941. https://doi.org/10.1002/2016RS006028
Milan SE, Lester M, Cowley SWH, Moen J, Sandholt PE, Owen CJ (1999) Meridian-scanning photometer, coherent hf radar, and magnetometer observations of the cusp: a case study. Annales Geophysicae 17(2):159–172. https://doi.org/10.1007/s00585-999-0159-5
Milan S, Lester M, Cowley S, Brittnacher M (2000) Convection and auroral response to a southward turning of the imf: Polar uvi, cutlass, and image signatures of transient magnetic flux transfer at the magnetopause. J Geophys Res Space Phys 105(A7):15741–15755
Millward GH, Moffett RJ, Balmforth HF, Rodger AS (1999) Modeling the ionospheric effects of ion and electron precipitation in the cusp. J Geophys Res Space Phys 104(A11):24603–24612. https://doi.org/10.1029/1999JA900249
Miyoshi Y, Oyama S, Saito S, Kurita S, Fujiwara H, Kataoka R, Ebihara Y, Kletzing C, Reeves G, Santolik O, Clilverd M, Rodger CJ, Turunen E, Tsuchiya F (2015) Energetic electron precipitation associated with pulsating aurora: Eiscat and van allen probe observations. J Geophys Res Space Phys 120(4):2754–2766
Moen J, Carlson HC, Sandholt PE (1999) Continuous observation of cusp auroral dynamics in response to an imf by polarity change. Geophys Res Lett 26(9):1243–1246. https://doi.org/10.1029/1999GL900224
Moen J, Walker I, Kersley L, Milan S (2002) On the generation of cusp hf backscatter irregularities. J Geophys Res Space Phys 107(A4):3
Moen J, Oksavik K, Carlson H (2004) On the relationship between ion upflow events and cusp auroral transients. Geophys Res Lett 31(11):66
Moen J, Gulbrandsen N, Lorentzen D, Carlson H (2007) On the mlt distribution of f region polar cap patches at night. Geophys Res Lett 34(14):66
Moen J, Rinne Y, Carlson HC, Oksavik K, Fujii R, Opgenoorth H (2008) On the relationship between thin birkeland current arcs and reversed flow channels in the winter cusp/cleft ionosphere. J Geophys Res Space Phys 113(A9):66. https://doi.org/10.1029/2008JA013061
Moen J, Oksavik K, Abe T, Lester M, Saito Y, Bekkeng TA, Jacobsen KS (2012) First in-situ measurements of hf radar echoing targets. Geophys Res Lett 39(7):66. https://doi.org/10.1029/2012GL051407
Moen J, Oksavik K, Alfonsi L, Daabakk Y, Romano V, Spogli L (2013) Space weather challenges of the polar cap ionosphere. J Space Weather Space Clim 3:02. https://doi.org/10.1051/swsc/2013025
Moore TE, Brenneman KS, Chappell CR, Clemmons JH, Collinson GA, Cully C, Donovan E, Earle GD, Gershman DJ, Heelis RA, Kistler LM, Kepko L, Khazanov G, Knudsen DJ, Lessard M, MacDonald EA, Nicolls MJ, Pollock CJ, Pfaff R, Rowland DE, Sanchez E, Schunk RW, Semeter J, Strangeway RJ, Thayer J (2016) Future atmosphere–ionosphere–magnetosphere

coupling study requirements, pp 355–376. https://doi.org/10.1002/9781119066880.ch28
Moser C, LaBelle J, Hatch S, Moen JI, Spicher A, Takahashi T, Kletzing CA, Bounds S, Oksavik K, Sigernes F, Yeoman TK (2020) The cusp as a VLF saucer source: first rocket observations of long-duration VLF saucers on the dayside. Geophys Res Lett 48(2):66. https://doi.org/10.1029/2020GL090747
Newell PT, Meng C-I (1992) Mapping the dayside ionosphere to the magnetosphere according to particle precipitation characteristics. Geophys Res Lett 19(6):609–612. https://doi.org/10.1029/92GL00404
Nishimura Y, Sadler FB, Varney RH, Gilles R, Zhang SR, Coster AJ, Nishitani N, Otto A (2021) Cusp dynamics and polar cap patch formation associated with a small imf southward turning. J Geophys Res Space Phys 126(5):2020–029090. https://doi.org/10.1029/2020JA029090
Nishimura Y, Verkhoglyadova O, Deng Y, Zhang S-R (2022) Chapter 3—density, irregularity, and instability. In: Nishimura, Y, Verkhoglyadova O, Deng Y, Zhang S-R (eds) Cross-scale coupling and energy transfer in the magnetosphere–ionosphere–thermosphere system, pp 103–216. https://doi.org/10.1016/B978-0-12-821366-7.00001-9
Nishitani N, Ogawa T, Pinnock M, Freeman MP, Dudeney JR, Villain J-P, Baker KB, Sato N, Yamagishi H, Matsumoto H (1999) A very large scale flow burst observed by the superdarn radars. J Geophys Res Space Phys 104(A10):22469–22486. https://doi.org/10.1029/1999JA900241
Nishitani N, Ruohoniemi JM, Lester M, Baker JBH, Koustov AV, Shepherd SG, Chisham G, Hori T, Thomas EG, Makarevich RA et al (2019) Review of the accomplishments of mid-latitude super dual auroral radar network (superdarn) hf radars. Prog Earth Planet Sci 6(1):1–57
Oksavik K, Moen J, Carlson HC (2004) High-resolution observations of the small-scale flow pattern associated with a poleward moving auroral form in the cusp. Geophys Res Lett 31(11):66. https://doi.org/10.1029/2004GL019838
Oksavik K, Moen J, Carlson H, Greenwald R, Milan S, Lester M, Denig W, Barnes R (2005) Multi-instrument mapping of the small-scale flow dynamics related to a cusp auroral transient. In: Annales Geophysicae, vol 23. Copernicus GmbH, pp 2657–2670
Oksavik K, Ruohoniemi J, Greenwald R, Baker J, Moen J, Carlson H, Yeoman TK, Lester M (2006) Observations of isolated polar cap patches by the European incoherent scatter (eiscat) svalbard and super dual auroral radar network (superdarn) Finland radars. J Geophys Res Space Phys 111(A5):66
Oksavik K, Moen JI, Rekaa EH, Carlson HC, Lester M (2011) Reversed flow events in the cusp ionosphere detected by superdarn hf radars. J Geophys Res Space Phys 116(A12):66. https://doi.org/10.1029/2011JA016788
Oksavik K, Moen J, Lester M, Bekkeng TA, Bekkeng JK (2012) In situ measurements of plasma irregularity growth in the cusp ionosphere. J Geophys Res Space Phys 117(A11):66. https://doi.org/10.1029/2012JA017835
Oksavik K, van der Meeren C, Lorentzen DA, Baddeley L, Moen J (2015) Scintillation and loss of signal lock from poleward moving auroral forms in the cusp ionosphere. J Geophys Res Space Phys 120(10):9161–9175
Ossakow SL, Chaturvedi PK (1979) Current convective instability in the diffuse aurora. Geophys Res Lett 6(4):332–334. https://doi.org/10.1029/GL006i004p00332
Oughton EJ, Skelton A, Horne RB, Thomson AW, Gaunt CT (2017) Quantifying the daily economic impact of extreme space weather due to failure in electricity transmission infrastructure. Space Weather 15(1):65–83
Oyama S, Watkins BJ, Nozawa S, Maeda S, Conde M (2005) Vertical ion motion observed with incoherent scatter radars in the polar lower ionosphere. J Geophys Res Space Phys 110(A4):04302. https://doi.org/10.1029/2004JA010705
Palmroth M, Grandin M, Sarris T, Doornbos E et al (2021) Lower-thermosphere-ionosphere (lti) quantities: current status of measuring techniques and models. Annales Geophysicae 39(5):189–237
Partamies N, Tesema F, Bland E (2022) Appearance and precipitation characteristics of high-latitude pulsating aurora. Front Astron Space Sci. https://doi.org/10.3389/fspas.2022.923396
Pellinen-Wannberg A (2005) Meteor head echoes-observations and models. In: Annales Geophysicae, vol 23. Copernicus GmbH, pp 201–205
Pellinen-Wannberg A, Kero J, Häggström I, Mann I, Tjulin A (2016) The forthcoming eiscat_3d as an extra-terrestrial matter monitor. Planet Space Sci 123:33–40
PFISR (2022) homepage. https://amisr.com/amisr/about/about_pfisr/. Accessed 13 Oct 2022
Pilipenko VA, Chugunova OM, Engebretson MJ (2008) Pc3-4 ulf waves at polar latitudes. J Atmos Solar-Terr Phys 70(18):2262–2274. https://doi.org/10.1016/j.jastp.2008.09.006. Transport processes in the coupled solar wind-geospace system seen from a high-latitude vantage point
Pinnock M, Rodger AS, Dudeney J, Baker K, Newell P, Greenwald R, Greenspan M (1993) Observations of an enhanced convection channel in the cusp ionosphere. J Geophys Res Space Phys 98(A3):3767–3776
Pitout, F, Eglitis, P, Blelly, P-L (2003) High-latitude dayside ionosphere response to pc5 field line resonance. vol 21 (no 7). Copernicus GmbH, pp 1509–1520
Plane JM, Feng W, Dawkins EC (2015) The mesosphere and metals: chemistry and changes. Chem Rev 115(10):4497–4541
Prikryl P, Jayachandran P, Mushini S, Pokhotelov D, MacDougall J, Donovan E, Spanswick E, St-Maurice J-P (2010) Gps tec, scintillation and cycle slips observed at high latitudes during solar minimum, vol 28 (no 6). Copernicus GmbH, pp 1307–1316
Provan G, Yeoman T, Milan S (1998) CUTLASS Finland radar observations of the ionospheric signatures of flux transfer events and the resulting plasma flows. Annales Geophysicae 16(11):1411–1422
Rae I, Watt C, Fenrich F, Mann I, Ozeke L, Kale A (2007) Energy deposition in the ionosphere through a global field line resonance, vol 25 (no 12). Copernicus GmbH, pp 2529–2539
Rankin R, Gillies D, Degeling A (2021) On the relationship between shear Alfven waves, auroral electron acceleration, and field line resonances. Space Sci Rev 217(4):1–35
Rapp M, Strelnikova I, Li Q, Engler N, Teiser G (2013) Charged aerosol effects on the scattering of radar waves from the d-region. Climate and weather of the Sun-Earth System (CAWSES). Springer, Dordrecht, pp 339–363
Reay S, Allen W, Baillie O, Bowe J, Clarke E, Lesur V, Macmillan S (2005) Space weather effects on drilling accuracy in the north sea, vol 23 (no 9). Copernicus GmbH, pp 3081–3088
Rinne Y, Moen J, Oksavik K, Carlson HC (2007) Reversed flow events in the winter cusp ionosphere observed by the European Incoherent Scatter (EISCAT) Svalbard radar. J Geophys Res Space Phys 112(A10):66. https://doi.org/10.1029/2007JA012366
RISR (2022) homepage. https://amisr.com/amisr/about/resolute-bay-isrs/. Accessed 13 Oct 2022
Samson J (1991) Geomagnetic pulsations and plasma waves in the earth's magnetosphere. Geomagnetism 4:481–592
Sarris TE (2019) Understanding the ionosphere thermosphere response to solar and magnetospheric drivers: status, challenges and open issues. Philos Trans 377:66
Sato K, Tsutsumi M, Sato T, Nakamura T, Saito A, Tomikawa Y, Nishimura K, Kohma M, Yamagishi H, Yamanouchi T (2014) Program of the *Antarctic syowa* mst/is radar (pansy). J Atmos Solar Terr Phys 118:2–15. https://doi.org/10.1016/j.jastp.2013.08.022
Semeter J, Butler T, Heinselman C, Nicolls M, Kelly J, Hampton D (2009) Volumetric imaging of the auroral ionosphere: initial results from pfisr. J Atmos Solar Terr Phys 71(6):738–743. https://doi.org/10.1016/j.jastp.2008.08.014
Semeter J, Mrak S, Hirsch M, Swoboda J, Akbari H, Starr G, Hampton D, Erickson P, Lind F, Coster A et al (2017) Gps signal corruption by the discrete aurora: precise measurements from the Mahali experiment. Geophys Res Lett 44(19):9539–9546
Seppälä A, Matthes K, Randall CE, Mironova IA (2014) What is the solar influence on climate? Overview of activities during CAWSES-II. Prog Earth Planet Sci 1(1):24
Seppälä A, Clilverd MA, Beharrell MJ, Rodger CJ, Verronen PT, Andersson ME, Newnham DA (2015) Substorm-induced energetic electron precipitation: impact on atmospheric chemistry. Geophys Res Lett 42(19):8172–8176
Simon A (1963) Instability of a partially ionized plasma in crossed electric and magnetic fields. Phys Fluids 6(3):382–388. https://doi.org/10.1063/1.1706743
SIOS (2022) homepage. https://sios-svalbard.org/. Accessed 13 Oct 2022
Sivadas N, Semeter J, Nishimura Y, Kero A (2017) Simultaneous measurements of substorm-related electron energization in the ionosphere and the plasma sheet. J Geophys Res Space Phy 122(10):10528–10547

Skjæveland Å, Moen J, Carlson HC (2011) On the relationship between flux transfer events, temperature enhancements, and ion upflow events in the cusp ionosphere. J Geophys Res Space Phys 116(A10):66
Spicher A, Miloch WJ, Moen JI (2014) Direct evidence of double-slope power spectra in the high-latitude ionospheric plasma. Geophys Res Lett 41(5):1406–1412. https://doi.org/10.1002/2014GL059214
Spicher A, Cameron T, Grono EM, Yakymenko KN, Buchert SC, Clausen LBN, Knudsen DJ, McWilliams KA, Moen JI (2015) Observation of polar cap patches and calculation of gradient drift instability growth times: a swarm case study. Geophys Res Lett 42(2):201–206. https://doi.org/10.1002/2014GL062590
Spicher A, Ilyasov AA, Miloch WJ, Chernyshov AA, Clausen LBN, Moen JI, Abe T, Saito Y (2016) Reverse flow events and small-scale effects in the cusp ionosphere. J Geophys Res Space Phys 121(10):10466–10480. https://doi.org/10.1002/2016JA022999
Spicher A, Deshpande K, Jin Y, Oksavik K, Zettergren MD, Clausen LBN, Moen JI, Hairston MR, Baddeley L (2020) On the production of ionospheric irregularities via Kelvin–Helmholtz instability associated with cusp flow channels. J Geophys Res Space Phys 125(6):2019–027734. https://doi.org/10.1029/2019JA027734
Spicher A, LaBelle J, Bonnell JW, Roglans R, Moser C, Fuselier SA, Bounds S, Clausen LBN, Di Mare F, Feltman CA, Jin Y, Kletzing C, Miloch WJ, Moen JI, Oksavik K, Sawyer R, Takahashi T, Yeoman TK (2022) Interferometric study of ionospheric plasma irregularities in regions of phase scintillations and hf backscatter. Geophys Res Lett 49(12):2021–097013. https://doi.org/10.1029/2021GL097013
Spogli L, Alfonsi L, De Franceschi G, Romano V, Aquino MHO, Dodson A (2009) Climatology of gps ionospheric scintillations over high and mid-latitude European regions. Annales Geophysicae 27(9):3429–3437. https://doi.org/10.5194/angeo-27-3429-2009
SSF (2022) homepage. https://www.forskningsradet.no/en/svalbard-science-forum/. Accessed 13 Oct 2022
Stamm J, Vierinen J, Urco JM, Gustavsson B, Chau JL (2021) Radar imaging with eiscat 3d. In: Annales Geophysicae, vol 39. Copernicus GmbH, pp 119–134
Tesema F, Partamies N, Nesse Tyssøy H, McKay D (2020) Observations of precipitation energies during different types of pulsating aurora. Annales Geophysicae 38(6):1191–1202
Tesema F, Partamies N, Whiter DK, Ogawa Y (2022) Types of pulsating aurora: comparison of model and EISCAT electron density observations. Ann Geophys 40:1–10. https://doi.org/10.5194/angeo-40-1-2022
Toledo-Redondo S, André M, Aunai N, Chappell CR, Dargent J, Fuselier SA, Glocer A, Graham DB, Haaland S, Hesse M, Kistler LM, Lavraud B, Li W, Moore TE, Tenfjord P, Vines SK (2021) Impacts of ionospheric ions on magnetic reconnection and earth's magnetosphere dynamics. Rev Geophys 59(3):2020. https://doi.org/10.1029/2020RG000707
TRACERS (2022) homepage. https://tracers.physics.uiowa.edu/. Accessed 13 Oct 2022
Tsunoda RT (1988) High-latitude f region irregularities: a review and synthesis. Rev Geophys 26(4):719–760. https://doi.org/10.1029/RG026i004p00719
UK Government, Dept of Business Innovation and Skills (2015) Space weather preparedness strategy. https://assets.publishing.service.gov.uk/government/uploads/system/uploads/attachment_data/file/449593/BIS-15-457-space-weather-preparedness-strategy.pdf. Accessed 13 Oct 2022
UNIS (2022) homepage. https://www.unis.no/. Accessed 13 Oct 2022
US Department of Homeland Security (2019) Federal operating concept for impending space weather events. https://www.fema.gov/sites/default/files/2020-07/fema_incident-annex_space-weather.pdf. Accessed 13 Oct 2022
US NASEM (2022) homepage. https://science.nasa.gov/biological-physical/decadal-survey. Accessed 13 Oct 2022
Valentic T, Buonocore J, Cousins M, Heinselman C, Jorgensen J, Kelly J, Malone M, Nicolls M, Van Eyken A (2013) Amisr the advanced modular incoherent scatter radar. In: 2013 IEEE international symposium on phased array systems and technology. IEEE, pp 659–663
Van Eyken A, Rishbeth H, Willis D, Cowley S (1984) Initial EISCAT observations of plasma convection at invariant latitudes 70–77. J Atmos Terr Phys 46(6–7):635–641
Varney, R. homepage. http://landau.geo.cornell.edu/workshop_report.pdf. Accessed 13 Oct 2022
Verronen PT, Ulich T, Turunen E, Rodger CJ (2006) Sunset transition of negative charge in the D-region ionosphere during high-ionization conditions. Annales Geophysicae 24(1):187–202
Verronen PT, Andersson ME, Marsh DR, Kovács T, Plane JMC (2016) Waccm-d—whole atmosphere community climate model with d-region ion chemistry. J Adv Model Earth Syst 8:954–975. https://doi.org/10.1002/2015MS000592
Verronen PT, Kero A, Partamies N, Szelag ME, Oyama S-I, Miyoshi Y, Turunen E (2021) Simulated seasonal impact on middle atmospheric ozone from high-energy electron precipitation related to pulsating aurorae. Annales Geophysicae 39(5):883–897
Vickers H, Kosch MJ, Sutton E, Ogawa Y, La Hoz C (2013) Thermospheric atomic oxygen density estimates using the EISCAT Svalbard Radar. J Geophys Res Space Phys 118:1319–1330. https://doi.org/10.1002/jgra.50169
Vickers H, Kosch MJ, Sutton E, Bjoland L, Ogawa Y, La Hoz C (2014) A solar cycle of upper thermosphere density observations from the EISCAT Svalbard Radar. J Geophys Res Space Phys 119(8):6833–6845. https://doi.org/10.1002/2014JA019885
Vierinen, J, Markkanen, J, Krag, H (2009) High power large aperture radar observations of the iridium-cosmos collision. In: Proceedings of the 5th ESA space debris conference. Citeseer
Vierinen J, Markkanen J, Krag H, Siminski J, Mancas A (2017) Use of eiscat 3d for observations of space debris
Vierinen J, Chau JL, Charuvil H, Urco JM, Clahsen M, Avsarkisov V, Marino R, Volz R (2019) Observing mesospheric turbulence with specular meteor radars: a novel method for estimating second-order statistics of wind velocity. Earth Space Sci 6(7):1171–1195. https://doi.org/10.1029/2019EA000570
Wannberg G, Wolf I, Vanhainen L-G, Koskenniemi K, Röttger J, Postila M, Markkanen J, Jacobsen R, Stenberg A, Larsen R et al (1997) The EISCAT svalbard radar: a case study in modern incoherent scatter radar system design. Radio Sci 32(6):2283–2307
Weber EJ, Buchau J, Moore JG, Sharber JR, Livingston RC, Winningham JD, Reinisch BW (1984) F layer ionization patches in the polar cap. J Geophys Res Space Phys 89(A3):1683–1694. https://doi.org/10.1029/JA089iA03p01683
Wissing JM, Kallenrode M-B, Kieser J, Schmidt H, Rietveld MT, Strømme A, Erickson PJ (2011) Atmospheric ionization module Osnabrück (AIMOS): 3. Comparison of electron density simulations by AIMOS-HAMMONIA and incoherent scatter radar measurements. J Geophys Res Space Phys 116(A8):66
Woodman RF (1997) Coherent radar imaging: signal processing and statistical properties. Radio Sci 32(6):2373–2391
Yamauchi M (2019) Terrestrial ion escape and relevant circulation in space. Annales Geophysicae 37(6):1197–1222. https://doi.org/10.5194/angeo-37-1197-2019
Yamazaki Y, Kosch MJ, Ogawa Y (2017) Average field-aligned ion velocity over the EISCAT radars. J Geophys Res Space Phys 122(5):5630–5642. https://doi.org/10.1002/2017JA023974
Yau AW, Andre M (1997) Sources of ion outflow in the high latitude ionosphere. Space Sci Rev 80:1–25. https://doi.org/10.1023/A:1004947203046
Yue X, Wan W, Ning B, Jin L (2022) An active phased array radar in china. Nat Astron 6(5):619–619
Zhang Q-H, Zhang Y-L, Wang C, Lockwood M, Yang H-G, Tang B-B, Xing Z-Y, Oksavik K, Lyons LR, Ma Y-Z et al (2020) Multiple transpolar auroral arcs reveal insight about coupling processes in the earth's magnetotail. Proc Natl Acad Sci 117(28):16193–16198
Zhang H, Zong Q, Connor H, Delamere P, Facskó G, Han D, Hasegawa H, Kallio E, Kis Á, Le G et al (2022) Dayside transient phenomena and their impact on the magnetosphere and ionosphere. Space Sci Rev 218(5):1–146
Zou S, Ridley A, Jia X, Boyd E, Nicolls M, Coster A, Thomas E, Ruohoniemi J (2017) Pfisr observation of intense ion upflow fluxes associated with an sed during the 1 June 2013 geomagnetic storm. J Geophys Res Space Phys 122(2):2589–2604

Publisher's Note